

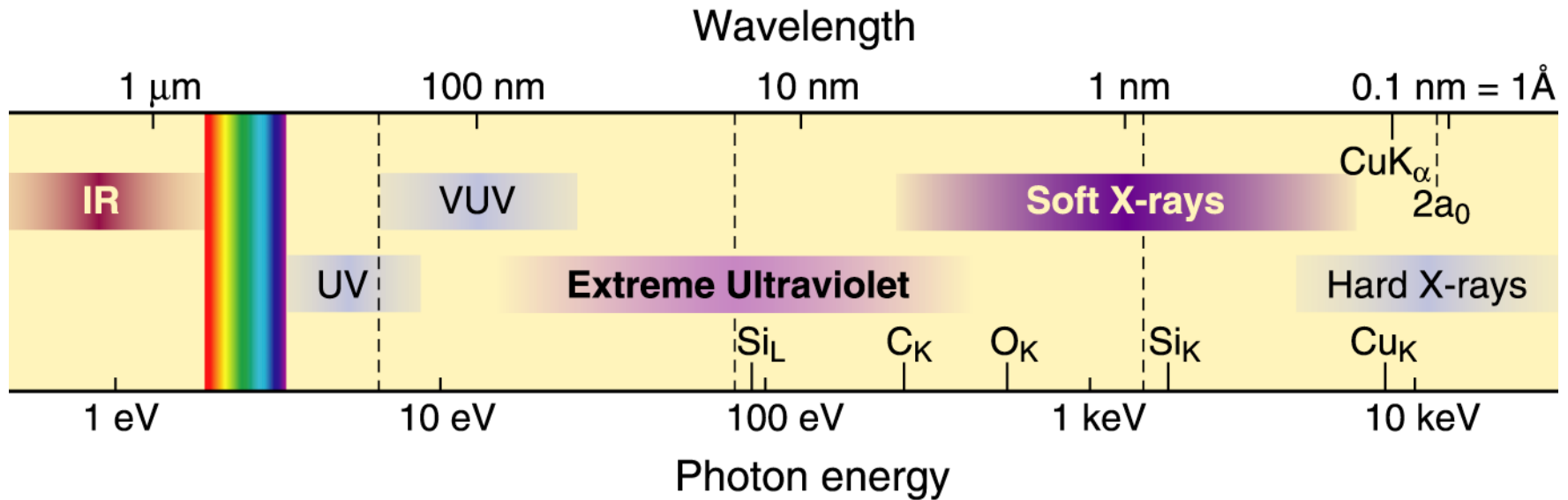


Soft and Hard X-Ray Microscopy

David Attwood
University of California, Berkeley

Cheiron School
September 2012
SPring-8

The short wavelength region of the electromagnetic spectrum



- See smaller features
- Write smaller patterns
- Elemental and chemical sensitivity

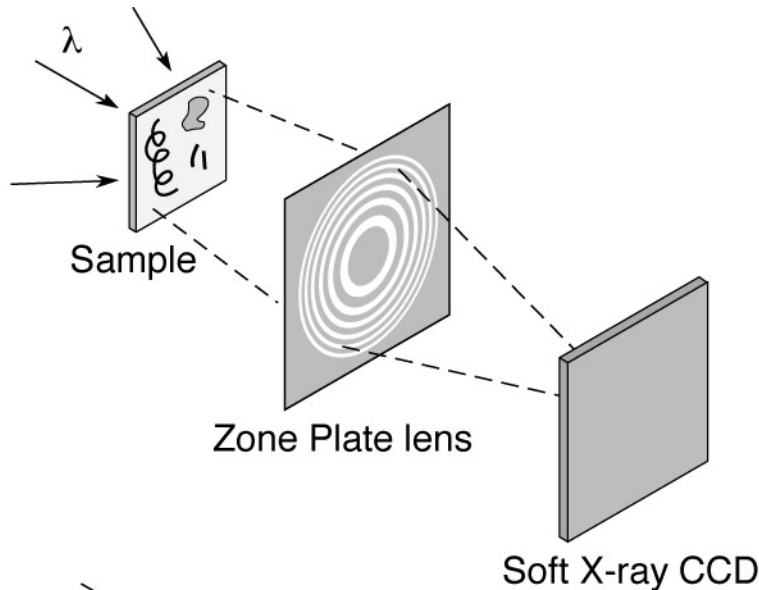
$$\hbar\omega \cdot \lambda = hc = 1239.842 \text{ eV nm}$$

$$n = 1 - \delta + i\beta \quad \delta, \beta \ll 1$$

Two common soft x-ray microscopes

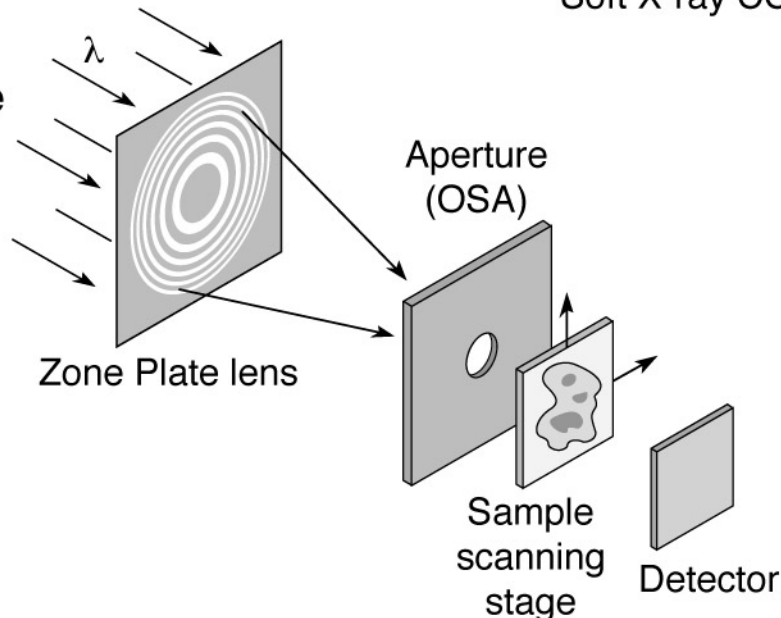


Full-Field Microscope



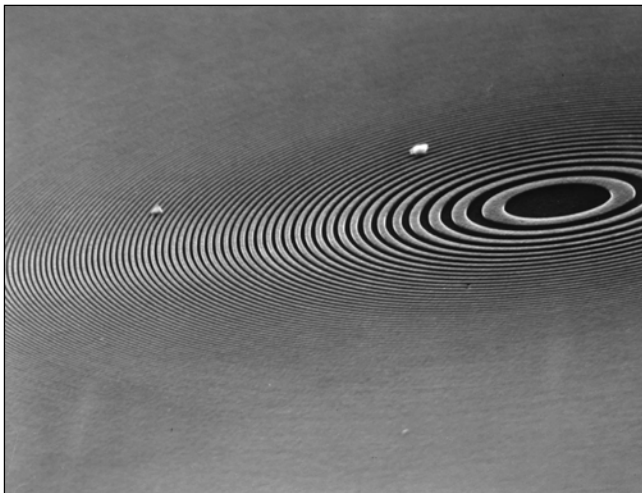
- 10–20 nm spatial resolution
- Modest spectral resolution
- Seconds exposure time
- Bending magnet radiation
- Higher radiation dose
- Flexible sample environment (wet, cryo, labeled magnetic fields, electric fields, cement, ...)

Scanning Microscope

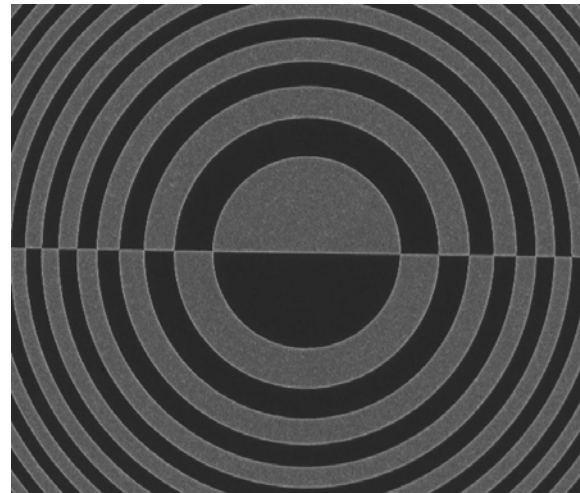


- 10–20 nm spatial resolution
- Least radiation dose
- Best spectral resolution
- Requires spatially coherent radiation
- Minutes exposure time
- Flexible sample environment
- Photoemission, fluorescence imaging

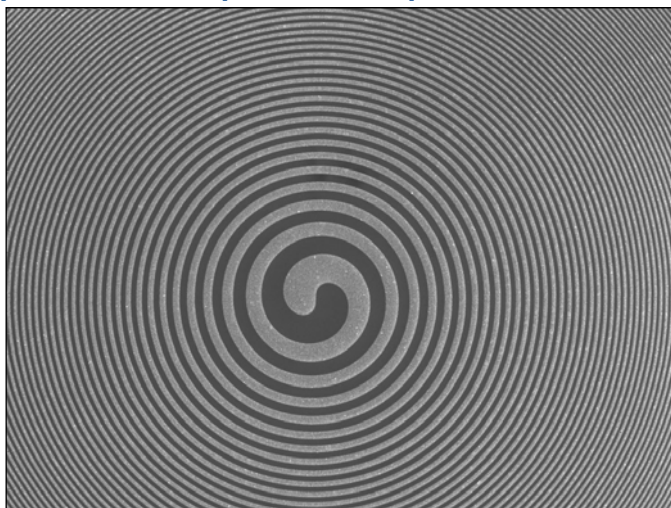
Soft x-ray zone plate



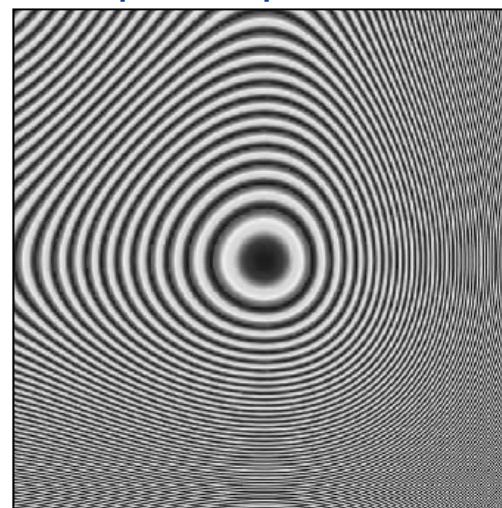
DIC microscopy



Spiral zone plate for phase contrast



Cubic phase plate for DOF



Courtesy of Anne Sakdinawat, Chang Chang, Weilun Chao and Erik Anderson (LBNL & UCB.)

Soft X-ray microscopy at a spatial resolution better than 15 nm

Weilun Chao^{1,2}, Bruce D. Harteneck¹, J. Alexander Liddle¹, Erik H. Anderson¹ & David T. Attwood^{1,2}

Analytical tools that have spatial resolution at the nanometre scale are indispensable for the life and physical sciences. It is desirable that these tools also permit elemental and chemical identification on a scale of 10 nm or less, with large penetration depths. A variety of techniques^{1–7} in X-ray imaging are currently being developed that may provide these combined capabilities. Here we report the achievement of sub-15-nm spatial resolution with a soft X-ray microscope—and a clear path to below 10 nm—using an overlay technique for zone plate fabrication. The microscope covers a spectral range from a photon energy of 250 eV (~5 nm wavelength) to 1.8 keV (~0.7 nm), so that primary K and L atomic resonances of elements such as C, N, O, Al, Ti, Fe, Co and Ni can be probed. This X-ray microscopy technique is therefore suitable for a wide range of studies: biological imaging in the water window^{8,9}; studies of wet environmental samples^{10,11}; studies of magnetic nanostructures with both elemental and spin-orbit sensitivity^{12–14}; studies that require viewing through thin windows, coatings or substrates (such as buried electronic devices in a silicon chip¹⁵); and three-dimensional imaging of cryogenically fixed biological cells^{9,16}.

The microscope XM-1 at the Advanced Light Source (ALS) in Berkeley¹⁷ is schematically shown in Fig. 1. The microscope type is similar to that pioneered by the Göttingen/BESSY group (ref. 18, and references therein). A 'micro' zone plate (MZP) projects a full-field image to an X-ray-sensitive CCD (charge-coupled device), typically in one or a few seconds, often with several hundred images per day. The field of view is typically 10 μ m, corresponding to a magnification of 2,500. The condenser zone plate (CZP), with a central stop, serves two purposes in that it provides partially coherent hollow-cone illumination², and, in combination with a pinhole, serves as the

monochromator. Monochromatic radiation of $\lambda/\Delta\lambda = 500$ is used. Both zone plates are fabricated in-house, using electron beam lithography¹⁹.

The spatial resolution of a zone plate based microscope is equal to $k_1\lambda/NA_{MZF}$, where λ is the wavelength, NA_{MZF} is the numerical aperture of the MZP, and k_1 is an illumination dependent constant, which ranges from 0.3 to 0.61. For a zone plate lens used at high magnification, $NA_{MZF} = \lambda/2\Delta r_{MZF}$ where Δr_{MZF} is the outermost (smallest) zone width of the MZP²⁰. For the partially coherent illumination^{21,22} used here, $k_1 \approx 0.4$ and thus the theoretical resolution is $0.8\Delta r_{MZF}$, as calculated using the SPLAT computer program²³ (a two-dimensional scalar diffraction code, which evaluates partially coherent imaging). In previous results with a $\Delta r_{MZF} = 25$ nm zone plate, we reported² an unambiguous spatial resolution of 20 nm. Here we describe the use of an overlay nanofabrication technique that allows us to fabricate zone plates with finer outer zone widths, to $\Delta r_{MZF} = 15$ nm, and to achieve a spatial resolution of below 15 nm, with clear potential for further extension.

This technique overcomes nanofabrication limits due to electron beam broadening in high feature density patterning. Beam broadening results from electron scattering within the recording medium (resist), leading to a loss of image contrast and thus resolvability for

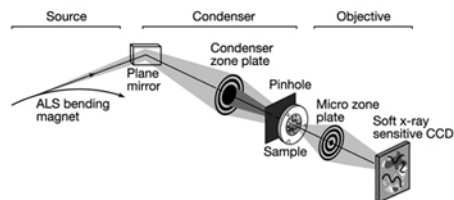


Figure 1 | A diagram of the soft X-ray microscope XM-1. The microscope uses a micro zone plate to project a full field image onto a CCD camera that is sensitive to soft X-rays. Partially coherent, hollow-cone illumination of the sample is provided by a condenser zone plate. A central stop and a pinhole provide monochromatization.

¹Center for X-ray Optics, Lawrence Berkeley National Laboratory, 1 Cyclotron Road, MS 2-400, ²Department of Electrical Engineering, California, Berkeley, California 94720, USA.

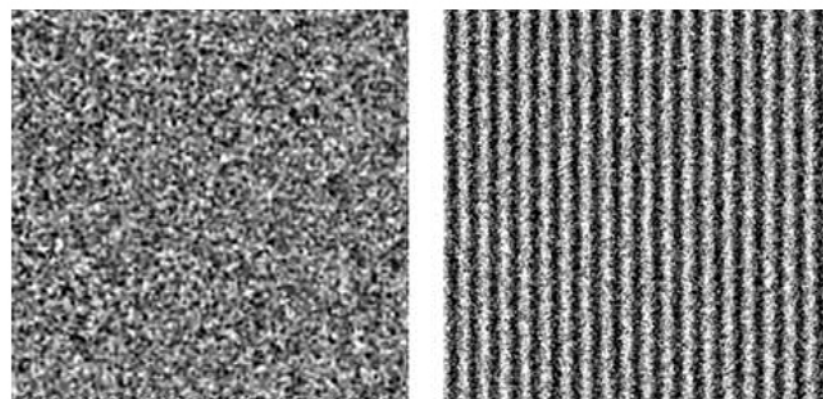
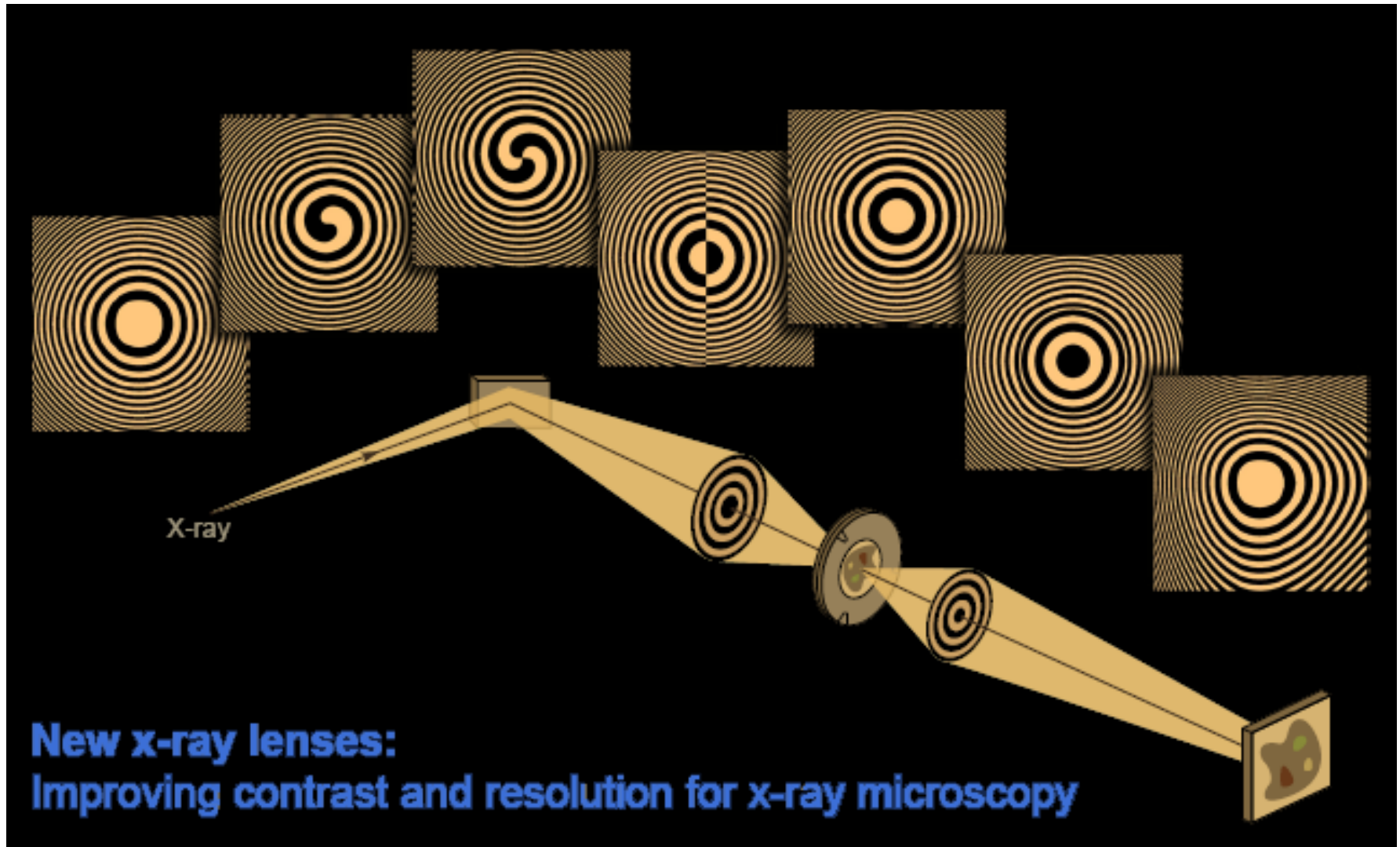


Figure 4 | Soft X-ray images of a 15.1 nm half-period test object, as formed with zone plates having outer zone widths of 25 nm and 15 nm.

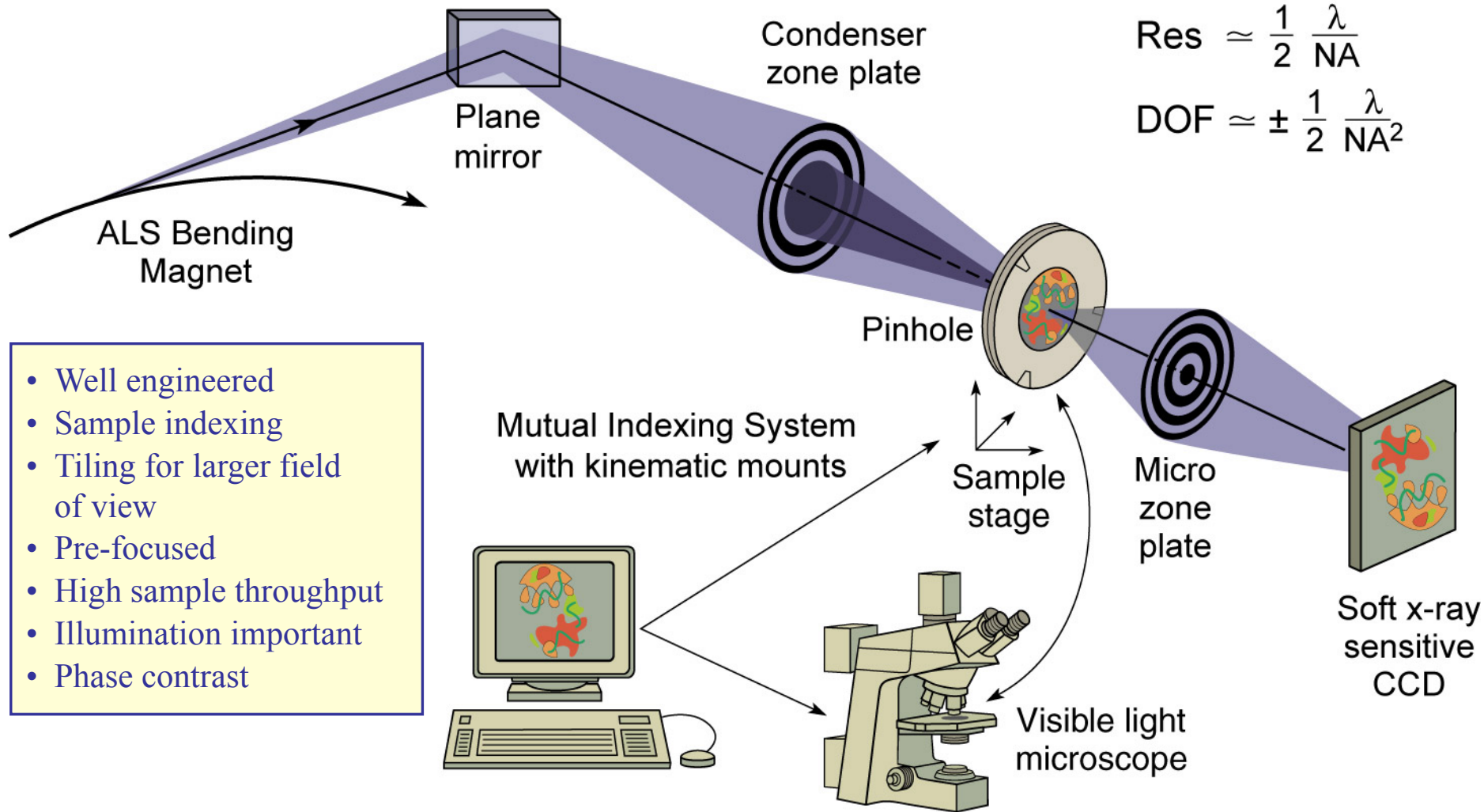
Cr/Si test pattern (Cr L₃ @ 574 eV)
(2000 X 2000, 10⁴ ph/pixel)

Novel zone plates for specific functionality



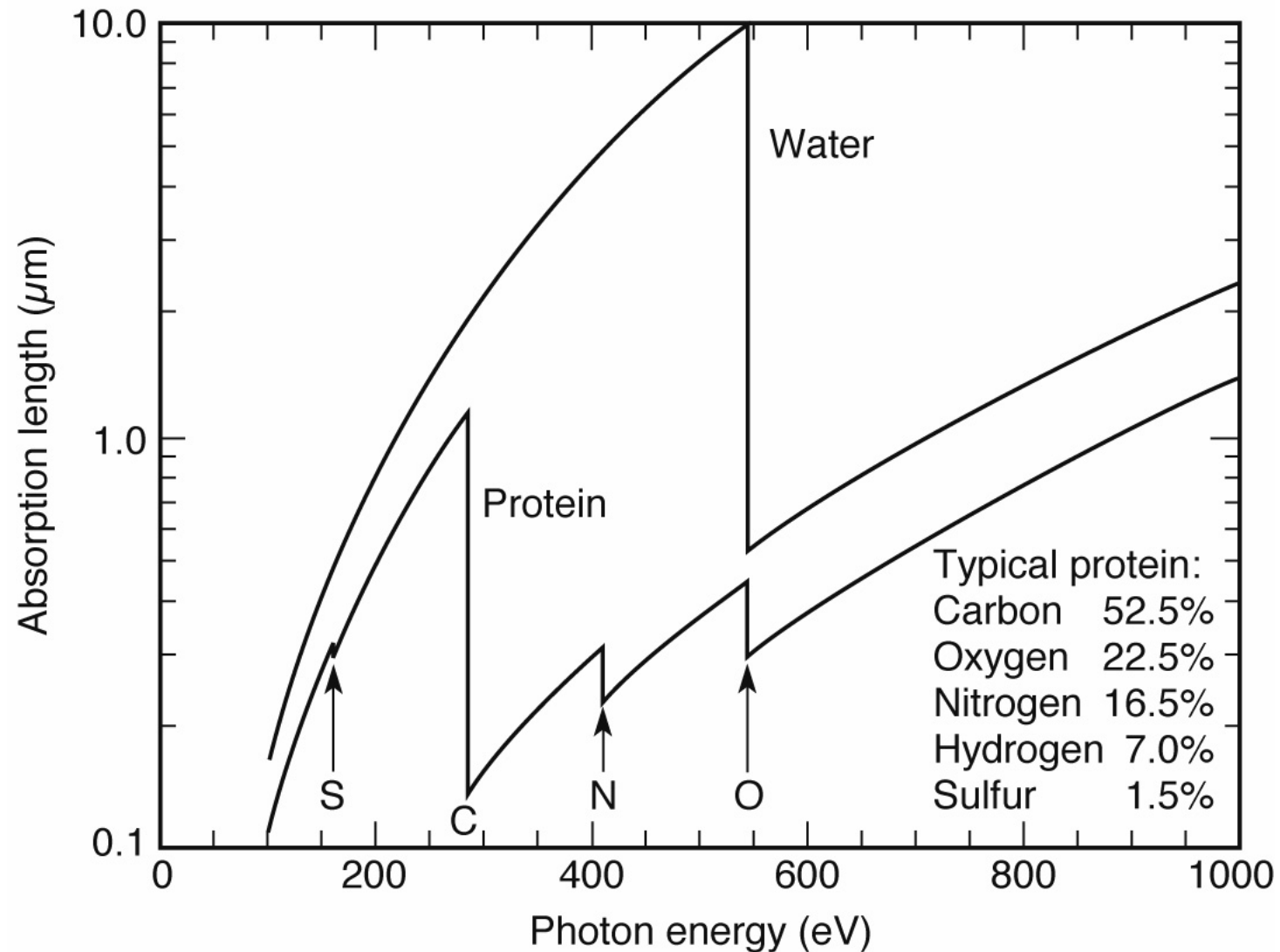
Courtesy of Anne Sakdinawat, UC Berkeley

High resolution zone plate microscopy



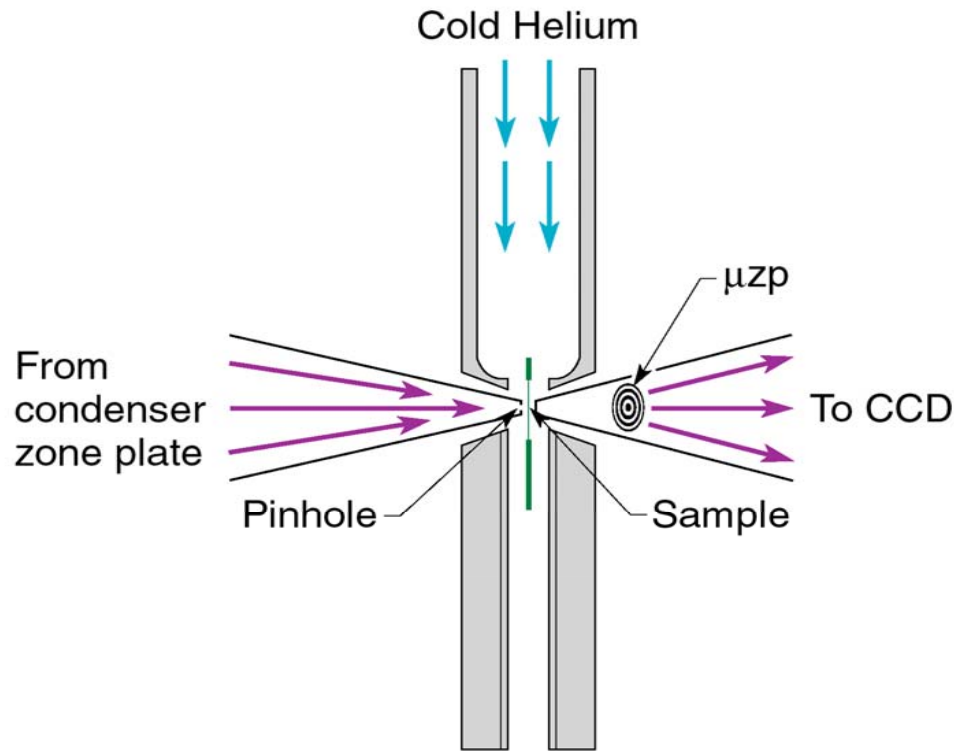
HiResZPMicrXM1Biology_Jan08.ai

The water window for biological x-ray microscopy



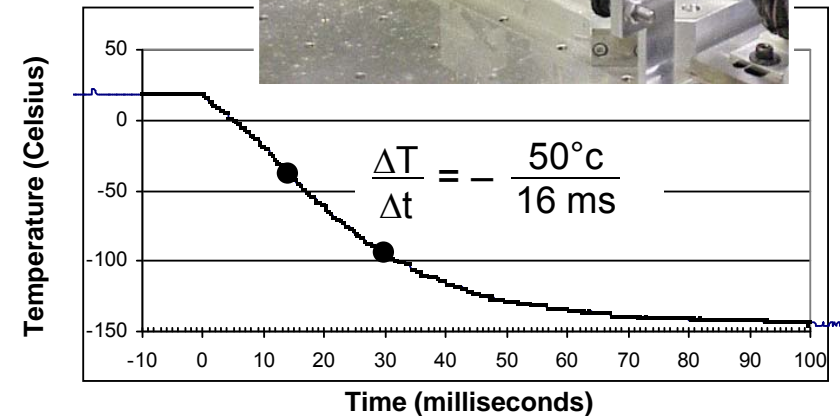
Ch09_F25VG.ai

Fast freeze cryo fixation strongly mitigates radiation dose effects



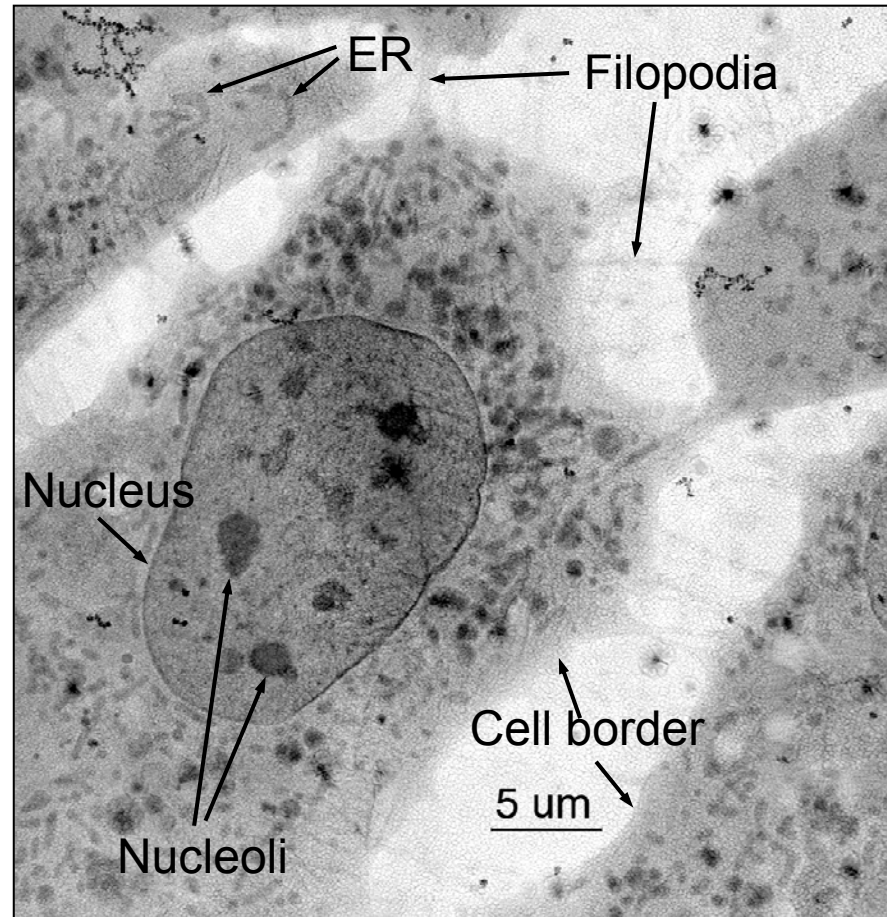
Helium passes through LN, is cooled, and directed onto sample windows

Fast Freeze



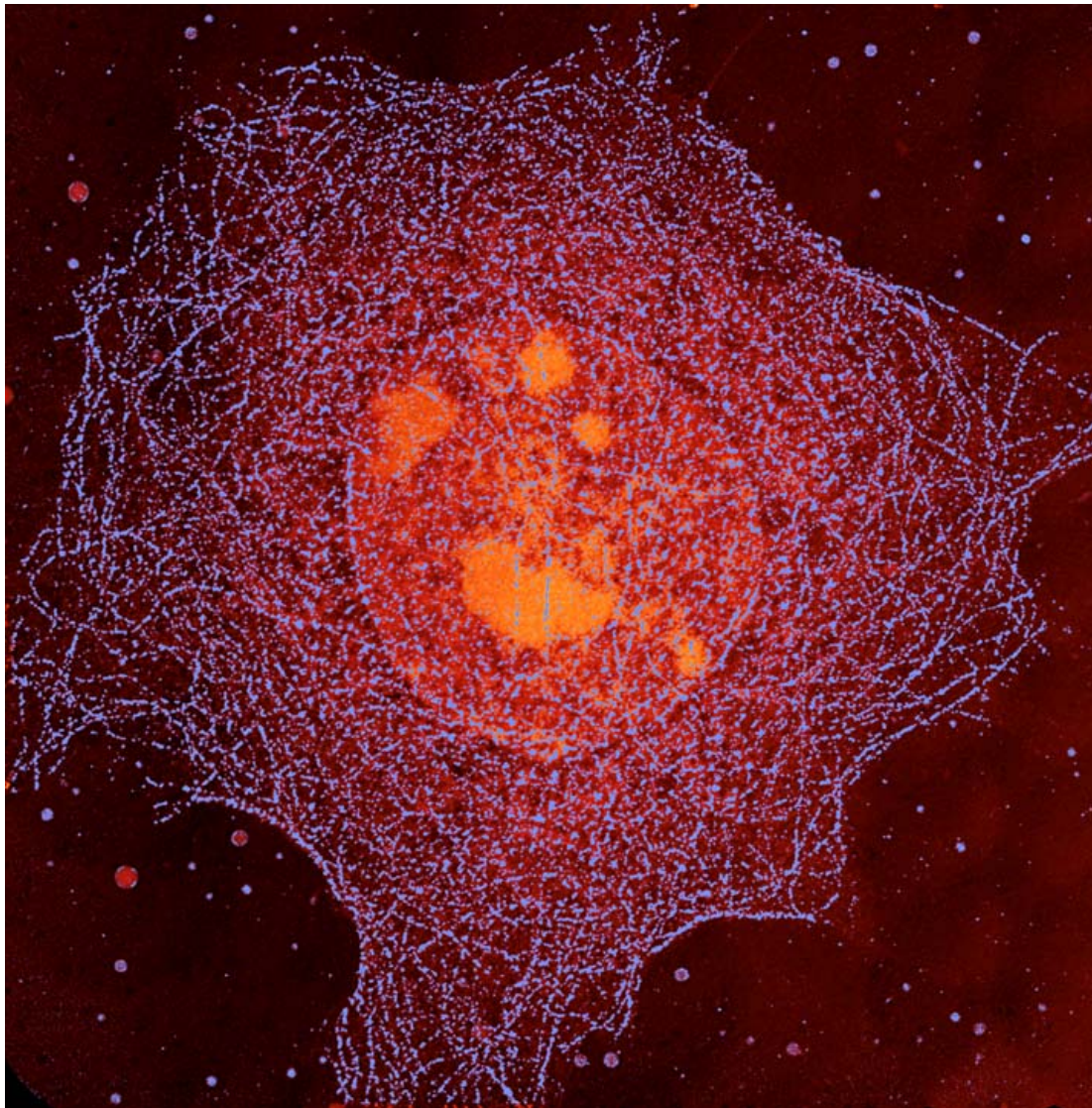
W. Meyer-Ilse, G. Denbeaux, L. Johnson, A. Pearson (CXRO-LBNL)

Cryo x-ray microscopy of 3T3 fibroblast cells



C. Larabell, D. Yager, D. Hamamoto, M. Bissell, T. Shin (LBNL Life Sciences Division)
W. Meyer-Ilse, G. Denbeaux, L. Johnson, A. Pearson (CXRO-LBNL)

Bending magnet radiation used with a soft x-ray microscope to form a high resolution image of a whole, hydrated mouse epithelial cell



$\hbar\omega = 520 \text{ eV}$

$32 \mu\text{m} \times 32 \mu\text{m}$

Ag enhanced Au labeling
of the microtubule network,
color coded blue.

Cell nucleus and nucleoli,
moderately absorbing,
coded orange.

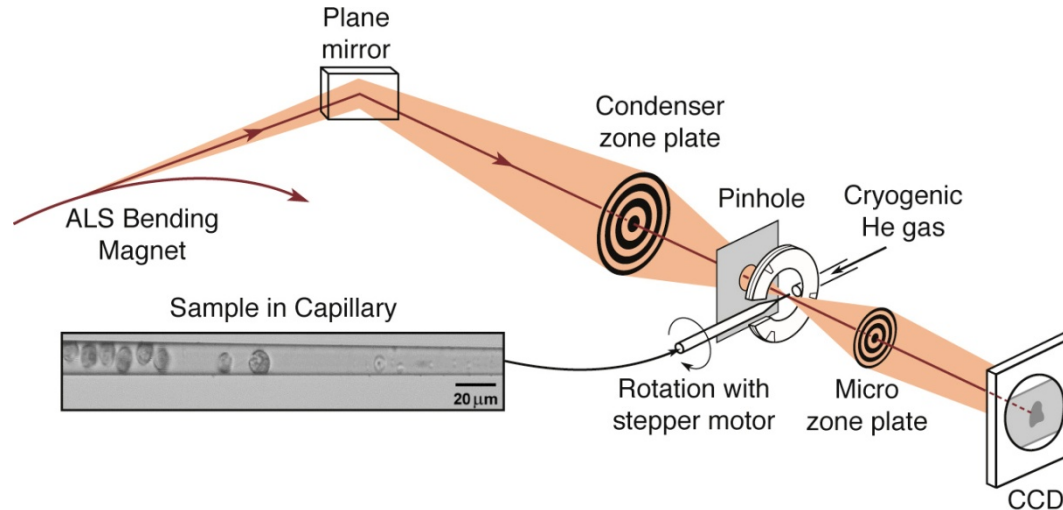
Less absorbing aqueous
regions coded black.

W. Meyer-Ilse et al.

J. Microsc. 201, 395 (2001)

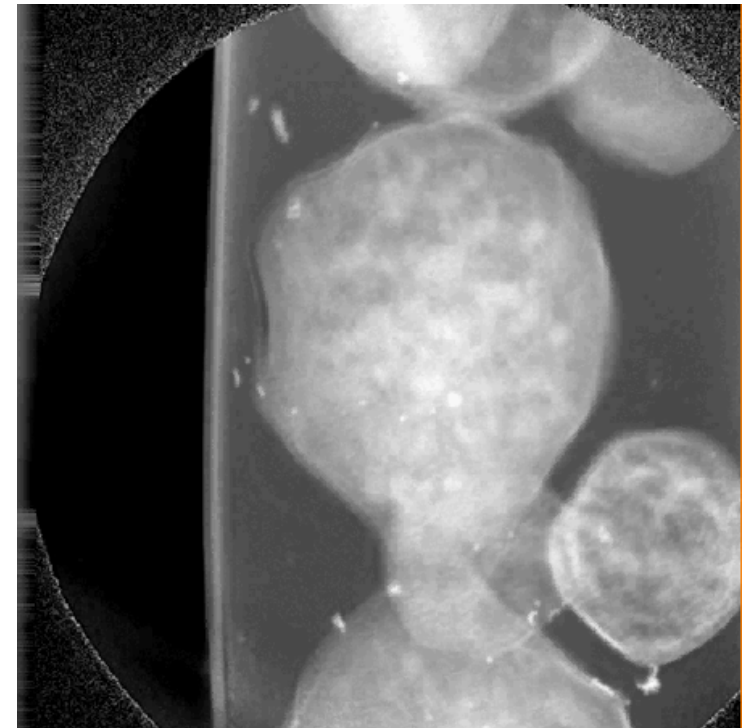
Courtesy of C. Larabell and W. Meyer-Ilse (LBNL)

Nanotomography of Cryogenic Fixed Cells



Courtesy of G. Schneider (BESSY)
Surf. Rev. Lett. 9, 177 (2002)

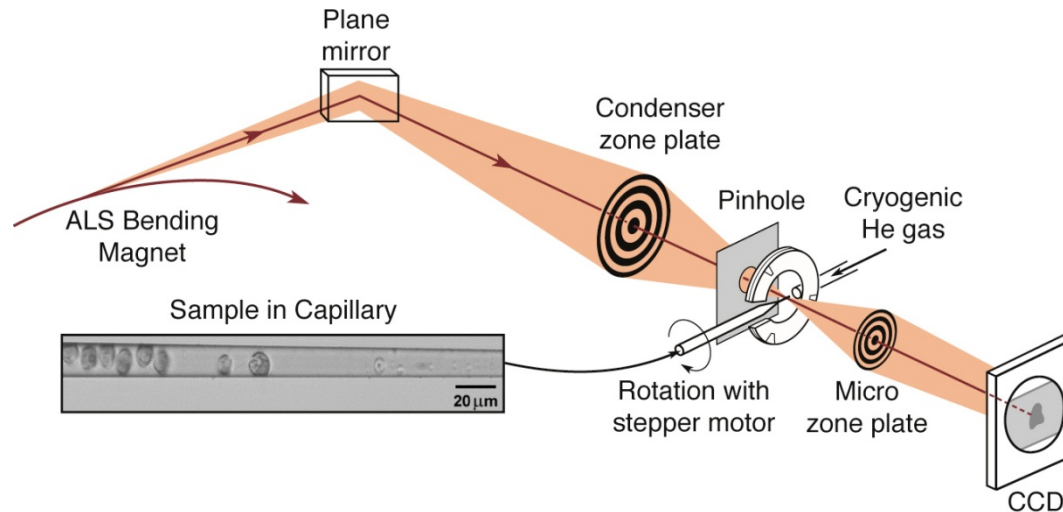
Soft X-Ray Nanotomography of a Yeast Cell



$\lambda = 2.4 \text{ nm}$

Courtesy of C. Larabell (UCSF & LBNL)
and M. LeGros (LBNL)

Nanotomography of Cryogenic Fixed Cells



$$\lambda = 2.4 \text{ nm (517 eV)}$$

$$\Delta r = 35 \text{ nm}$$

$$N = 320$$

$$NA = 0.034$$

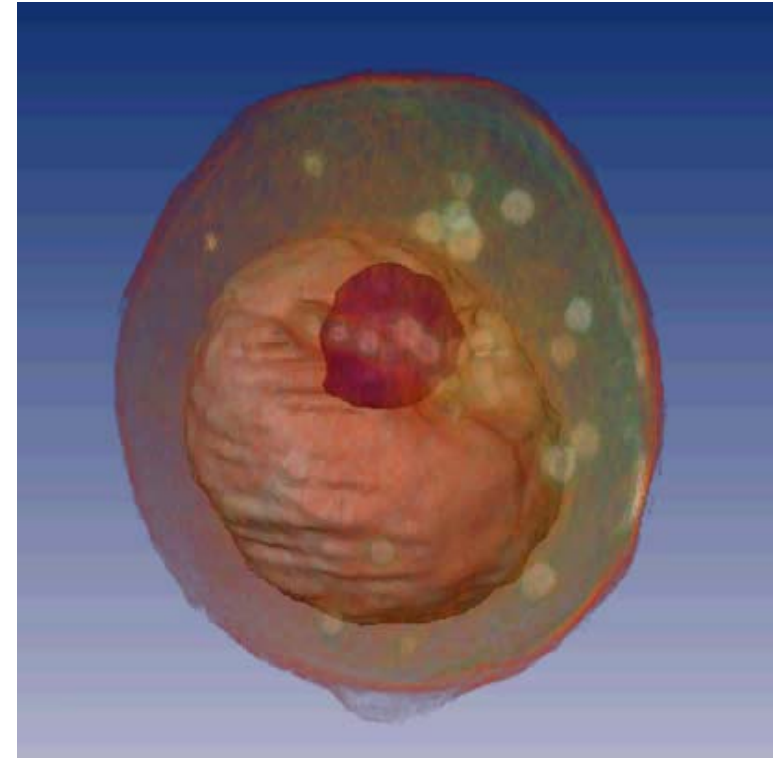
$$D = 45 \text{ } \mu\text{m}$$

$$f = 650 \text{ } \mu\text{m}$$

$$\sigma = 0.64$$

$$\text{Resolution} = 60 \text{ nm}$$

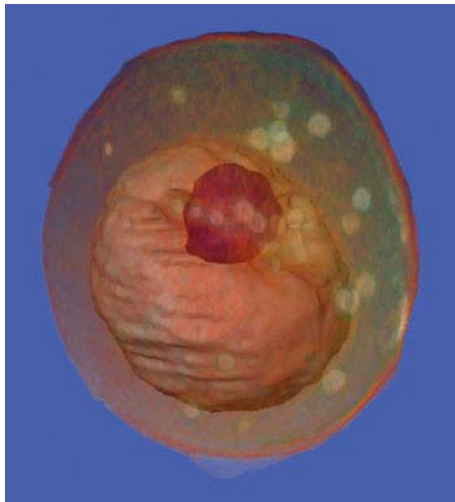
Soft X-Ray Nanotomography of a Yeast Cell



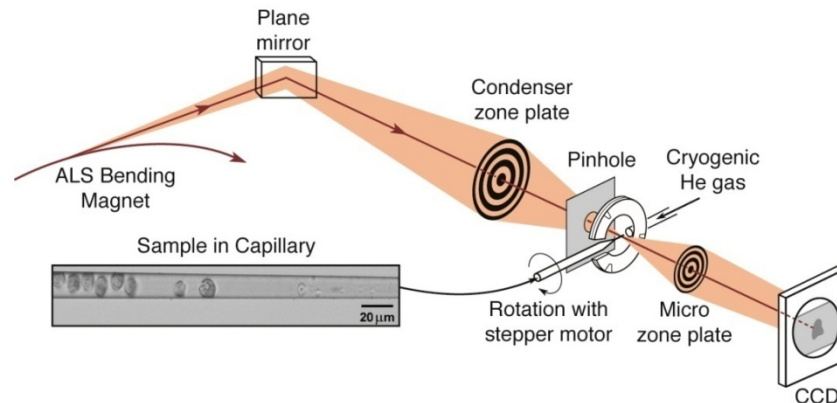
$$\lambda = 2.4 \text{ nm}$$

Courtesy of C. Larabell (UCSF & LBNL)
and M. LeGros (LBNL)

Small DOF limits resolution for thick samples



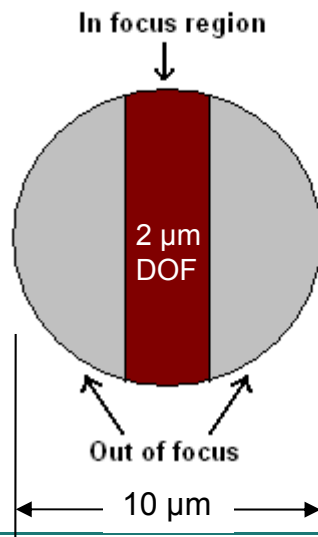
C. Larabell and M. LeGros,
Molec. Bio. Cell 15, 957 (2004)



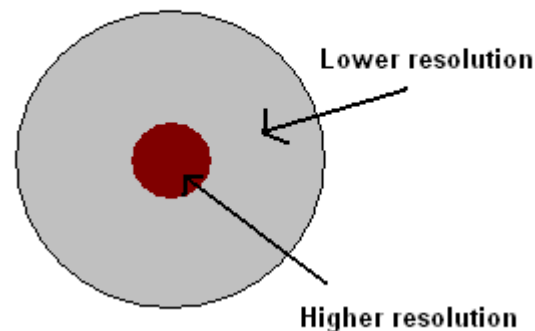
$$\text{Lateral Resolution} = \frac{k_1 \lambda}{NA} = 2k_1 \Delta r = \cancel{28} \text{ nm } 60 \text{ nm}$$

$$\text{Depth of field} = \pm \frac{1}{2} \frac{\lambda}{(NA)^2} = \pm \frac{2(\Delta r)^2}{\lambda} = 2 \mu\text{m}$$

Each projection image



Reconstructed image

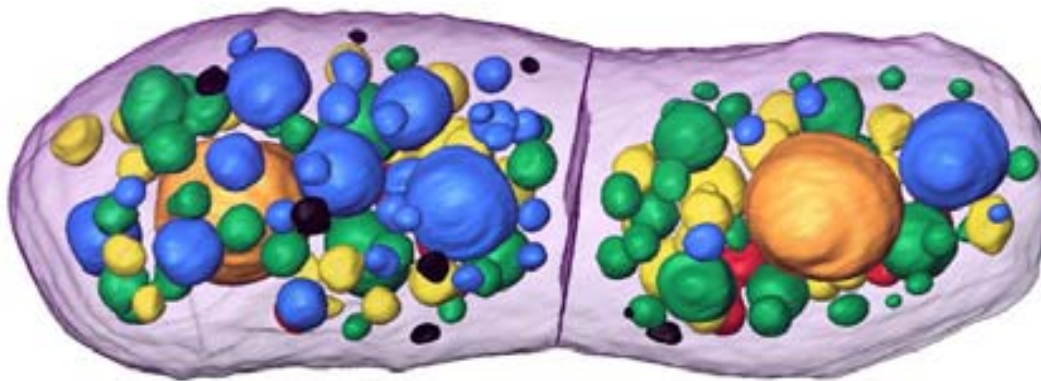


Courtesy of Anne Sakdinawat (LBNL & UCB.)

Mother daughter yeast cells just before separation



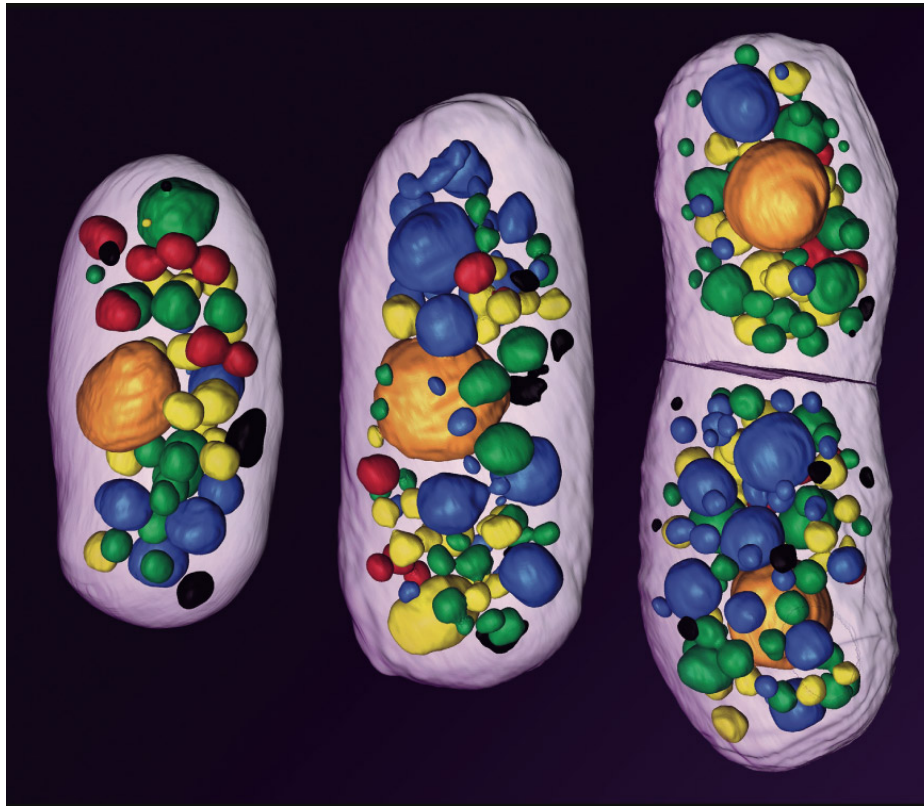
2-D slice from 3-D
Tomogram. Images
every 2°, 180° data
set, several minutes.
 $\Delta r = 45$ nm



Color coding
identifies subcellular
components by their
x-ray absorption
coefficients

Courtesy of Carolyn Larabell, UCSF/LBNL.

Biotomography at 60 nm resolution



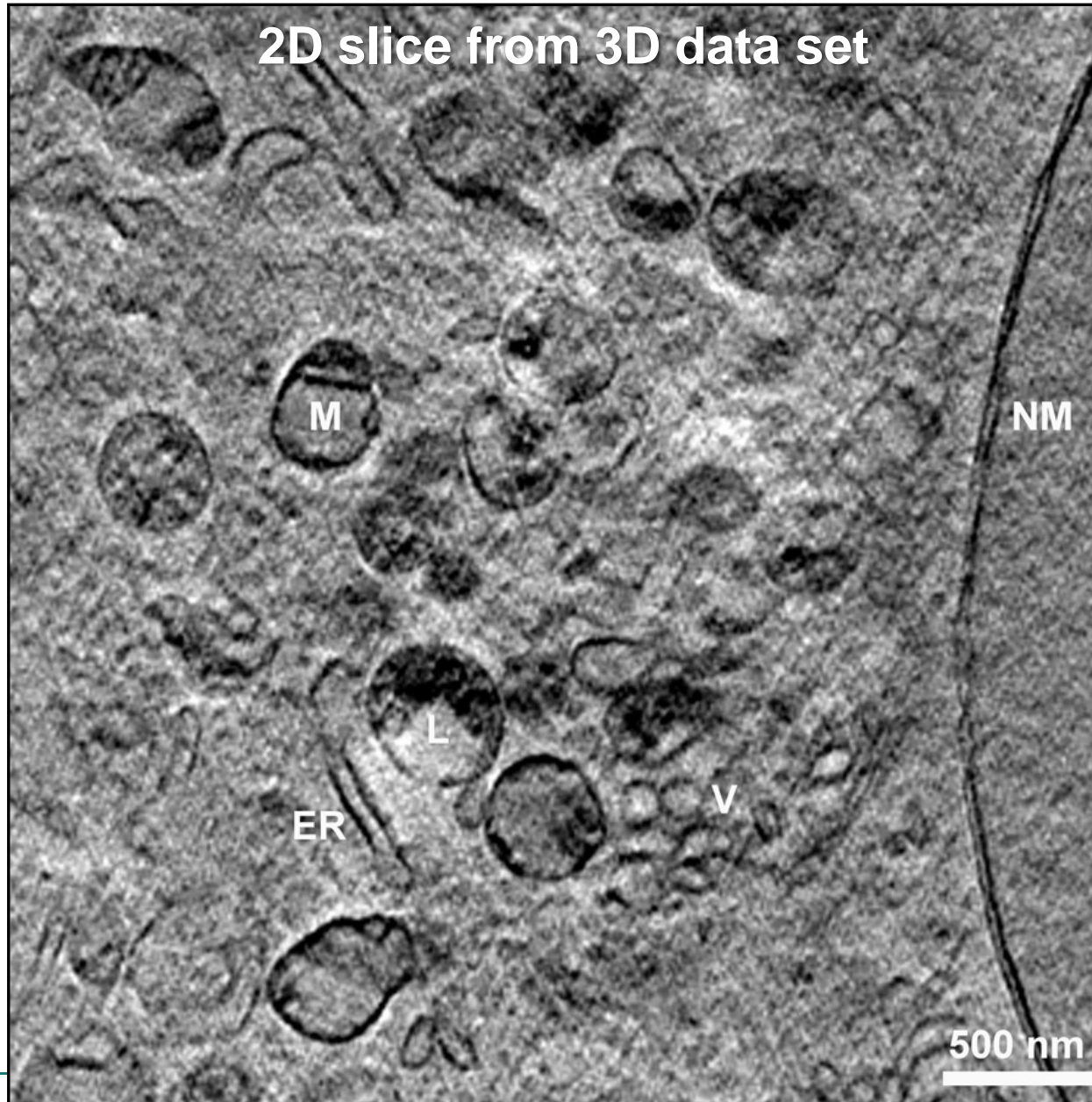
Courtesy of C. Larabell (UCSF & LBNL)

- Cryofixation
- 2° angular intervals
- Depth of focus limits resolution
- New XM-2 dedicated to biological applications, will become major facility worldwide to draw biologists to this evolving capability

UCSF NCXT

High resolution (29 nm), 3D image of a mouse cell by soft x-ray tomography

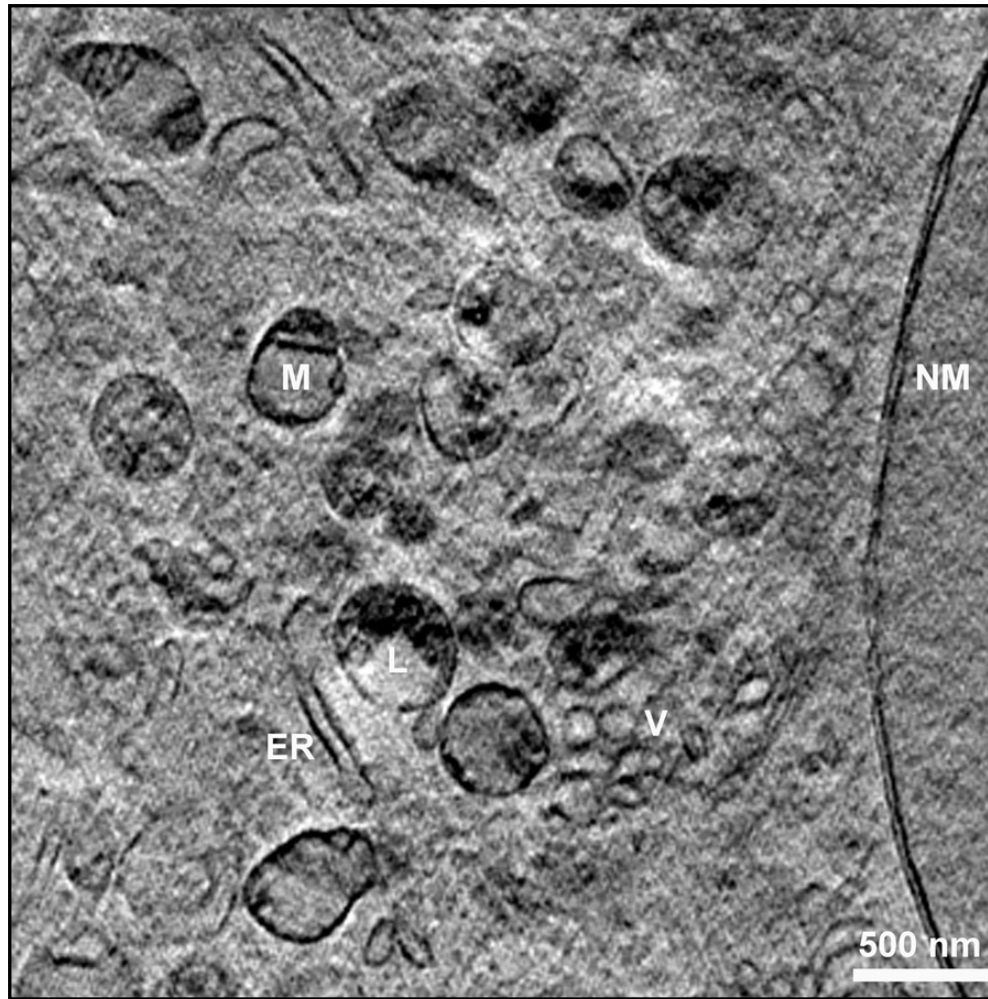
2D slice from 3D data set



517 eV (2.4 nm)
 $\Delta r = 25$ nm,
 1° intervals, $\pm 60^\circ$
29 nm nuclear
double membrane.

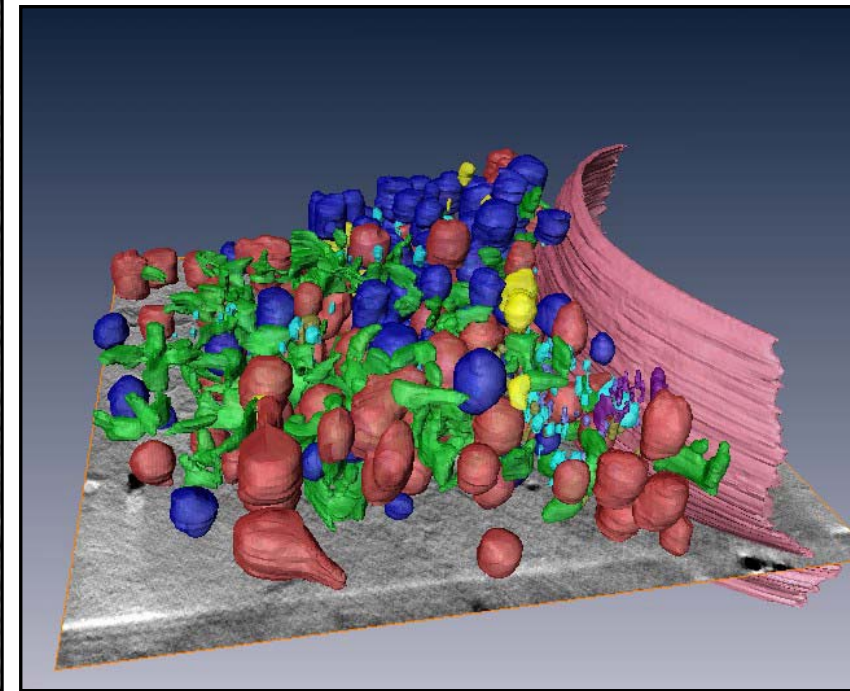
Courtesy of
Gerd Schneider, BESSYII
and James McNally, NIH.

2D slice from 3D data set



Details: 517 eV (2.4 nm)
 $\Delta r = 25$ nm, 1° intervals, $\pm 60^\circ$.
Note 29 nm nuclear membrane.

3D rendering



Courtesy of Gerd Schneider, BESSYII and James McNally, NIH.



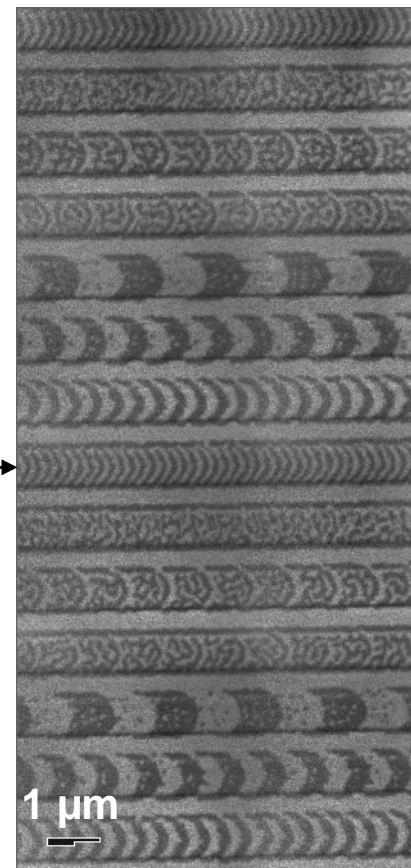
Magnetic x-ray microscopy using x-ray magnetic circular dichroism (XMCD)



Magnetic X-Ray Microscopy

- High spatial resolution in transmission
- Bulk sensitive (thin films)
- Complements surface sensitive PEEM
- Good elemental sensitivity
- Good spin-orbit sensitivity
- Allows applied magnetic field
- Insensitive to capping layers
- In-plane and out-of-plane measurements

100 nm
lines & spaces →



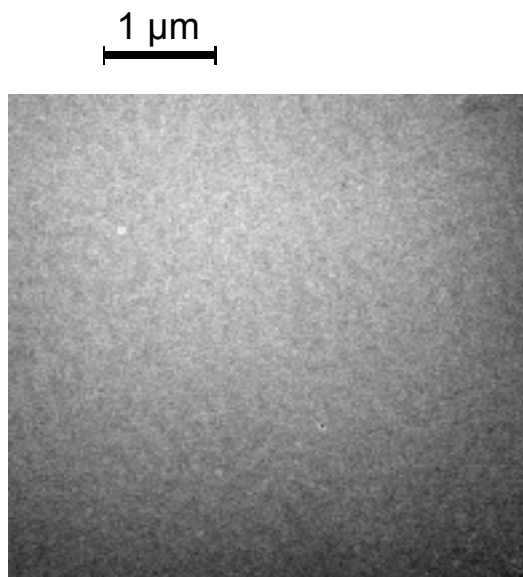
Courtesy of P. Fischer, (MPI, Stuttgart) and G. Denbeaux (CXRO/LBNL)



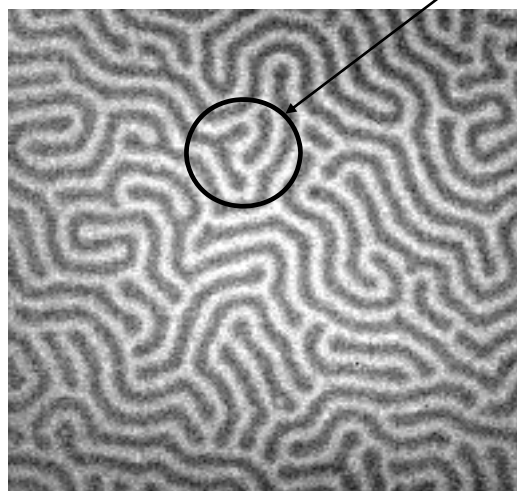
Magnetic domains imaged at different photon energies



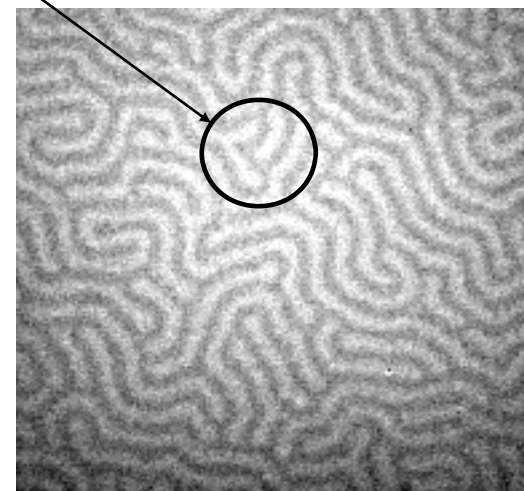
FeGd Multilayer



$\hbar\omega = 704 \text{ eV}$
below Fe L-edges



$\hbar\omega = 707.5 \text{ eV}$
Fe L₃-edge

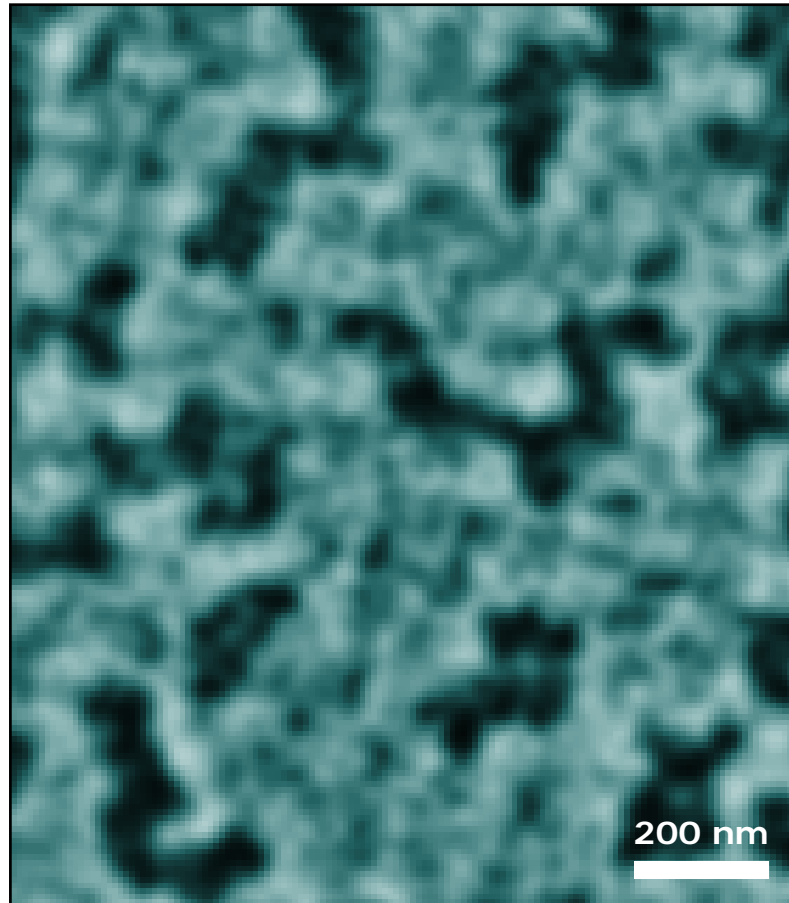


$\hbar\omega = 720.5 \text{ eV}$
Fe L₂-edge

Contrast reversal

P. Fischer, T. Eimüller, M. Koehler (U. Würzburg)
S. Tsunashima (U. Nagoya) and N. Tagaki (Sanyo)
G. Denbeaux, L. Johnson, A. Pearson (CXRO-LBNL)

Magnetic recording of nanomagnetic patterns to 15 nm spatial resolution



CoCrPt alloy
Co L_3 -edge at 778 eV
(1.59 nm)

Courtesy of Peter Fischer (LBNL)

P. Fischer et al., *Mat. Today* 9, 26 (2006).

Time resolved studies of vortex dynamics in patterned permalloy thin films

Pump and Probe setup requires:

- Pump: Current pulse to “pump” sample
- Probe: X-ray pulses (70ps) from ALS 2 Bunch mode
- Perfect repeatability of dynamics

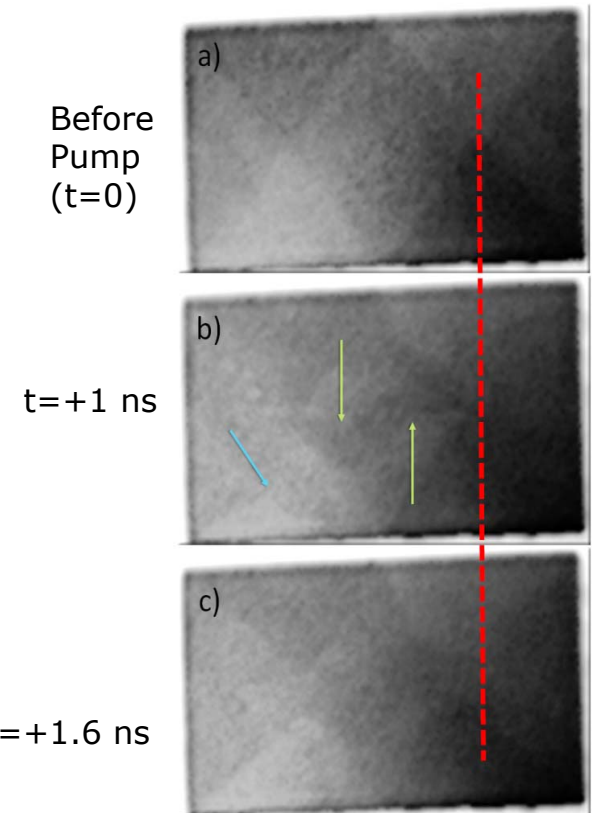


*B.L. Mesler, P. Fischer, W. Chao, E. H. Anderson,
D.H. Kim J. Vac. Sci. Technol. B 25, 2598 (2007).*

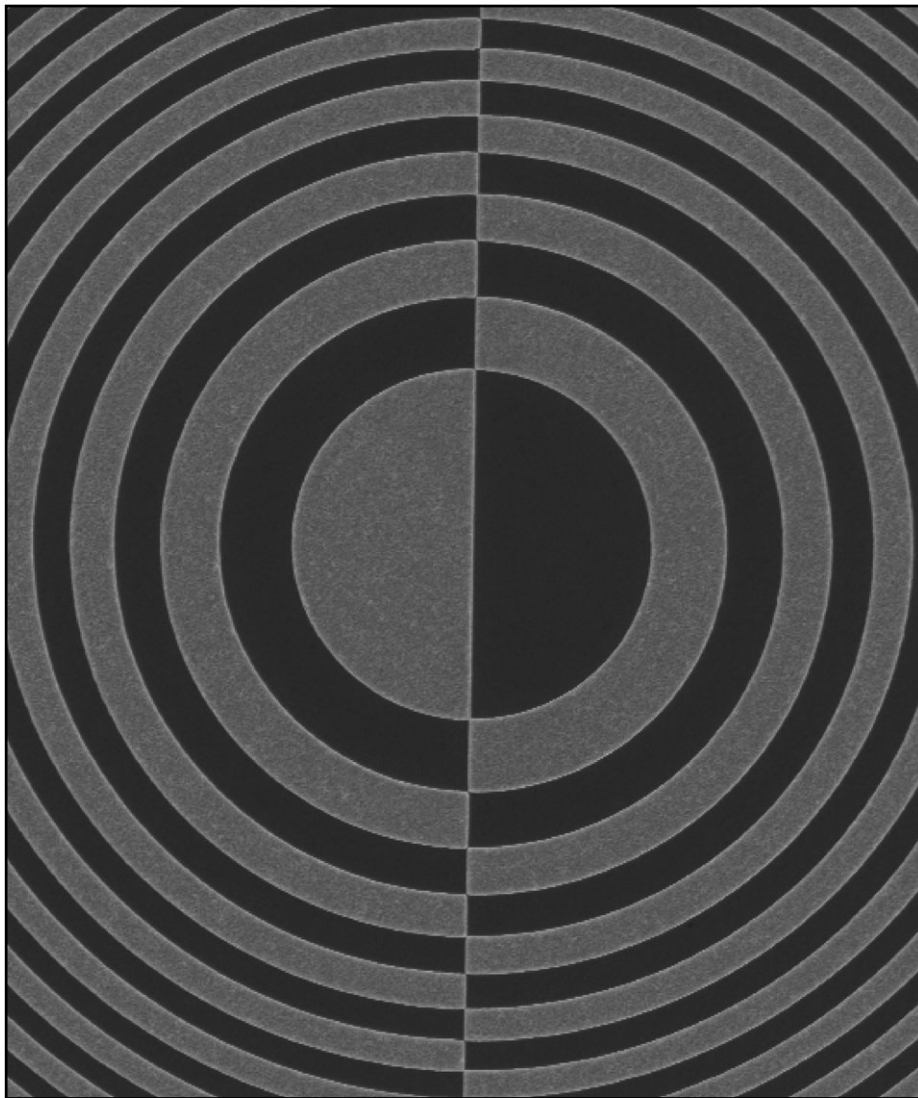
Sample:

50 nm thick $2\mu\text{m} \times 4\mu\text{m}$
permalloy ($\text{Ni}_{80}\text{Fe}_{20}$)

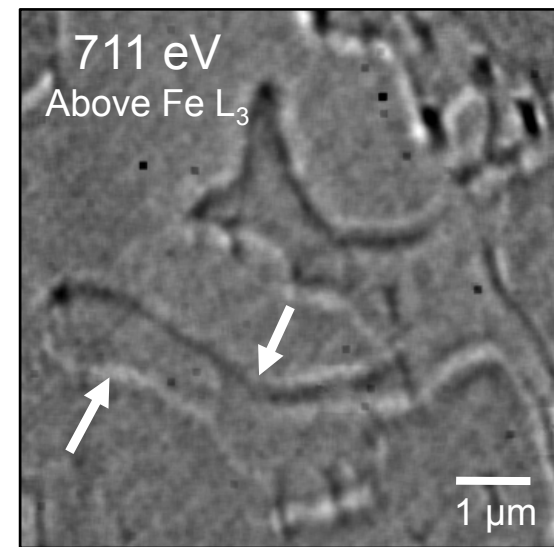
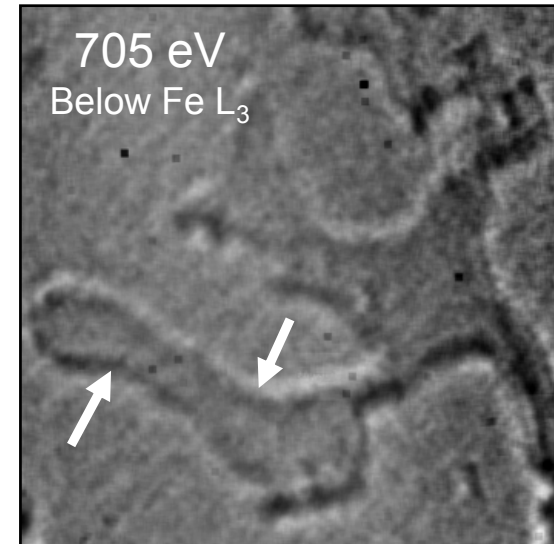
100nm thick gold waveguide
(ΔI along waveguide generates field to pump
sample)



Differential interference contrast (DIC) imaging at nanoscale magnetic edges



XOR Zone plate



59 nm thick Gd₂₅Fe₇₅ layer

Courtesy of A. Sakdinawat, C. Chang and P. Fischer.



Environmental Consequences of Portland cement

1.5 billion ton of cement

Generates 1.5 billion ton of CO₂

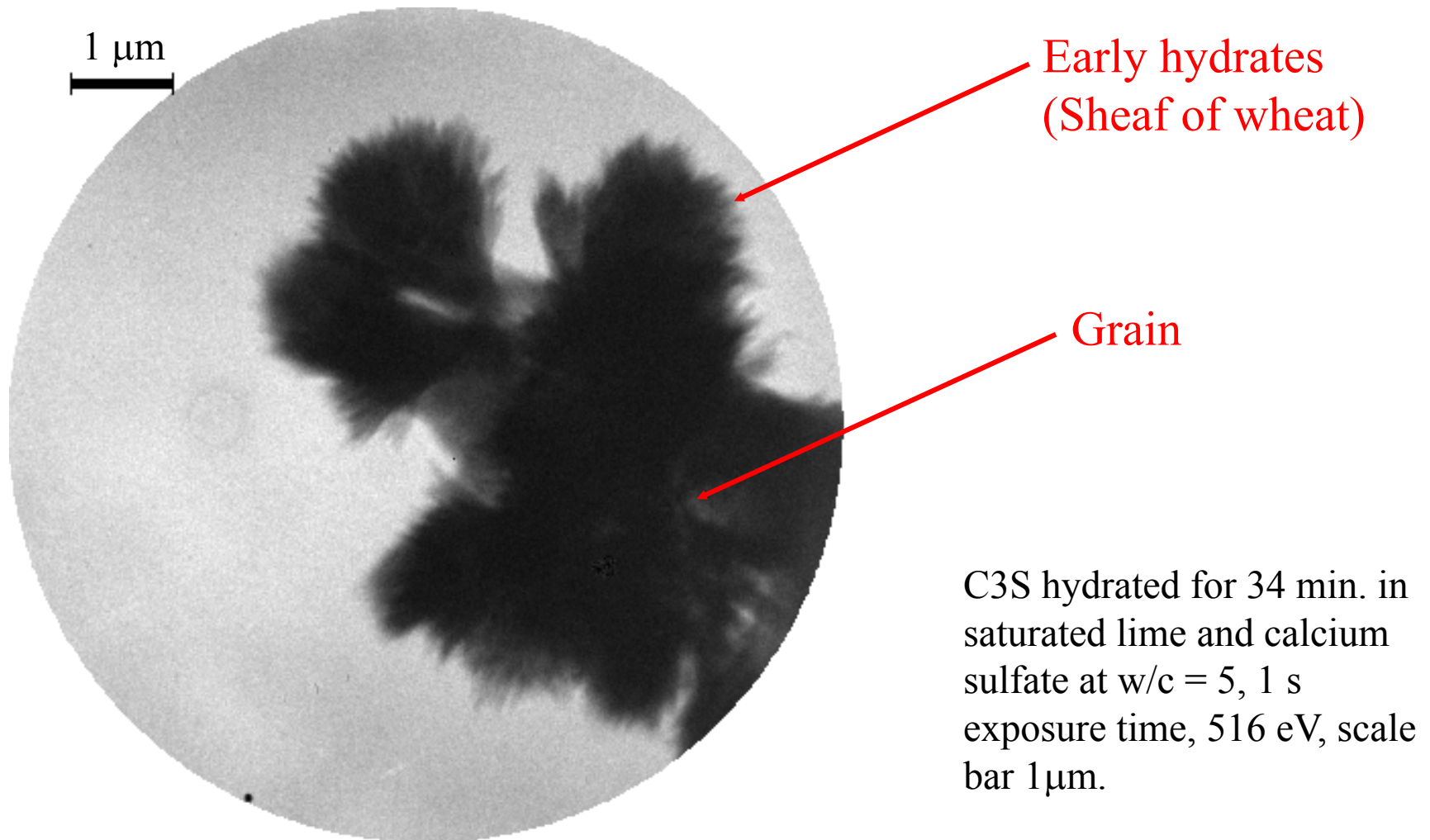
Responsible for 7% CO₂ production in the world

Problem!





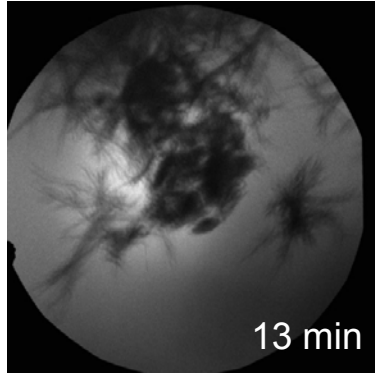
Nanoscale x-ray imaging of cement processes: early hydrates forming during the pre-induction period



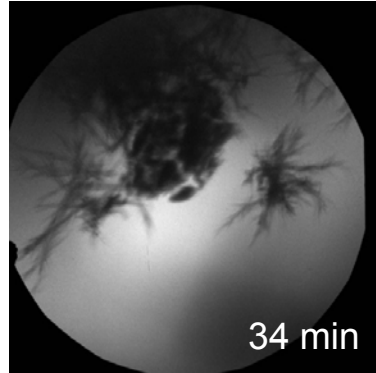
Nanoscale x-ray imaging of cement processes



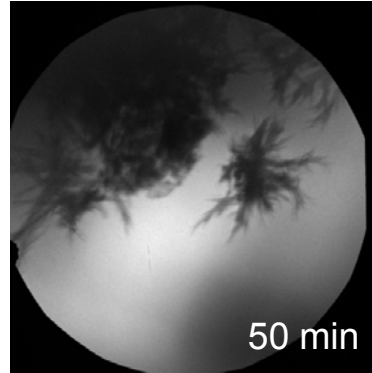
Calcium-Silicate-Hydrate (C-S-H): critical to cement strength and durability.



13 min

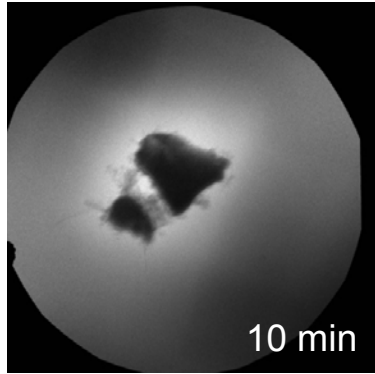


34 min

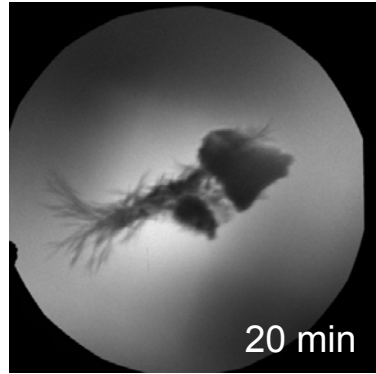


50 min

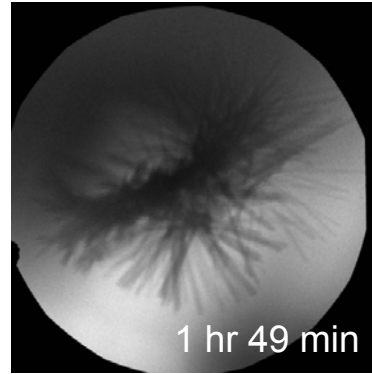
Orth C_3A



10 min

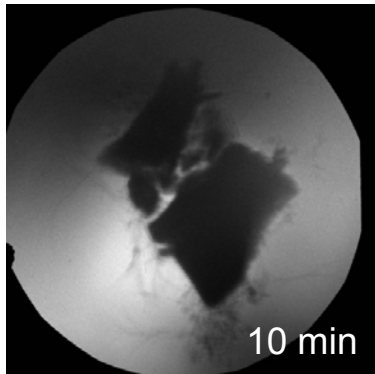


20 min

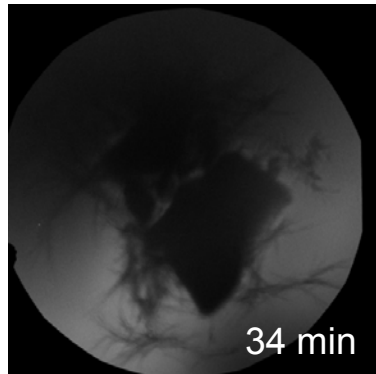


1 hr 49 min

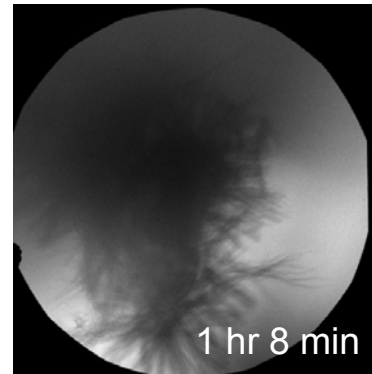
Orth C_3A + 1% $CaCl_2$



10 min



34 min



1 hr 8 min

Orth C_3A + accelerator

C: carbon

Ca: calcium

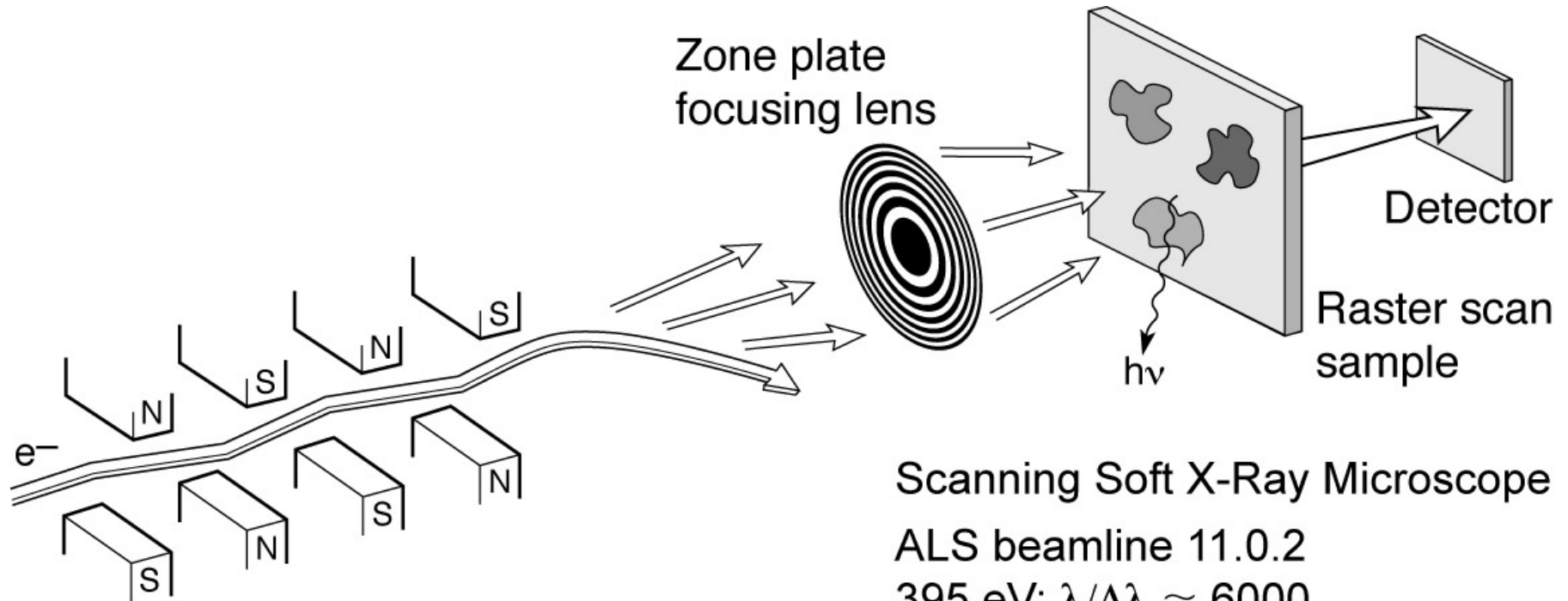
A: alumina (Al_2O_3)

S: silica (SiO_2)

Courtesy of Professor Paulo Monteiro, CEE, UC Berkeley

520 eV, 40 nm - spatial resolution

Spectromicroscopy: high spatial and high spectral resolution of surface and thin films



Scanning Soft X-Ray Microscope

ALS beamline 11.0.2

395 eV; $\lambda/\Delta\lambda \approx 6000$

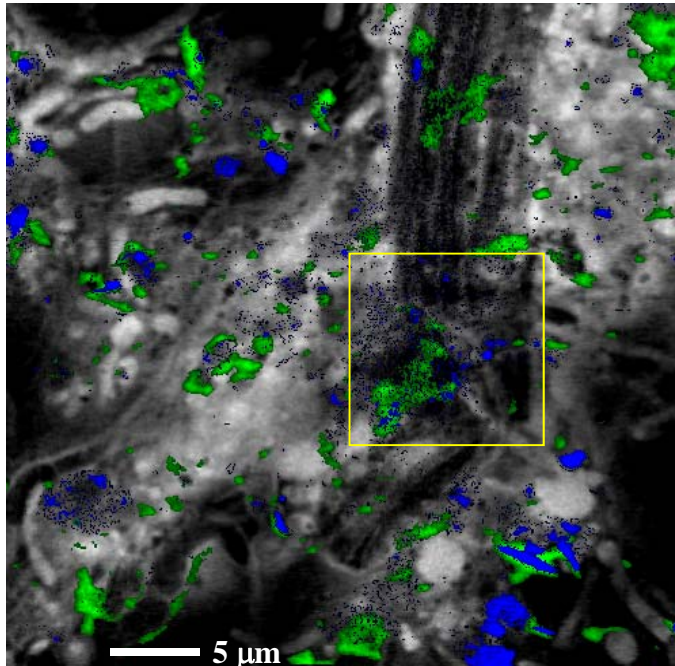
240 × 240 pixels

1.2 μm × 1.2 μm

2 ms dwell time

Ch09_F40a_Feb2010.ai

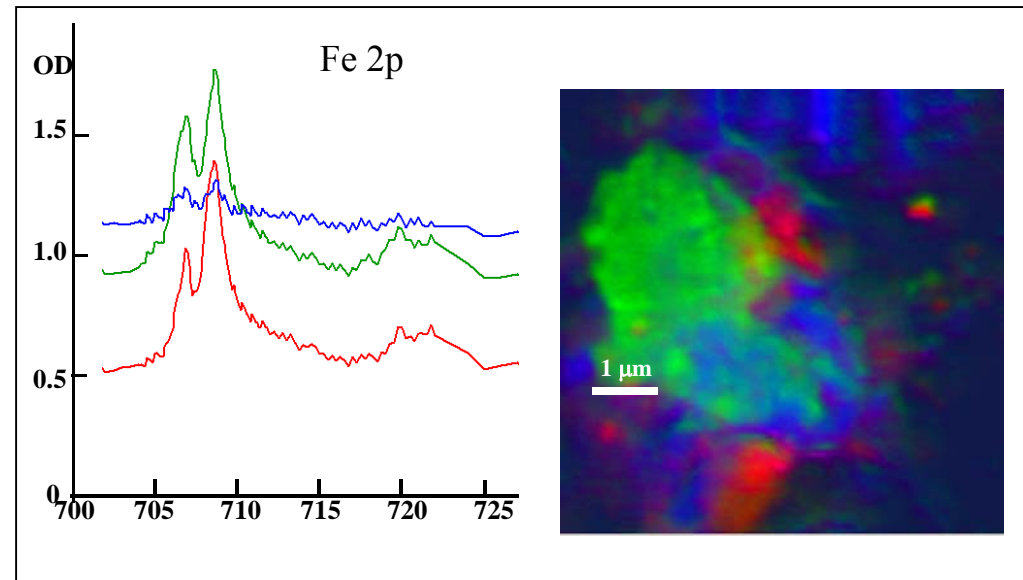
Biofilm from Saskatoon River



Protein (gray), Ca, K

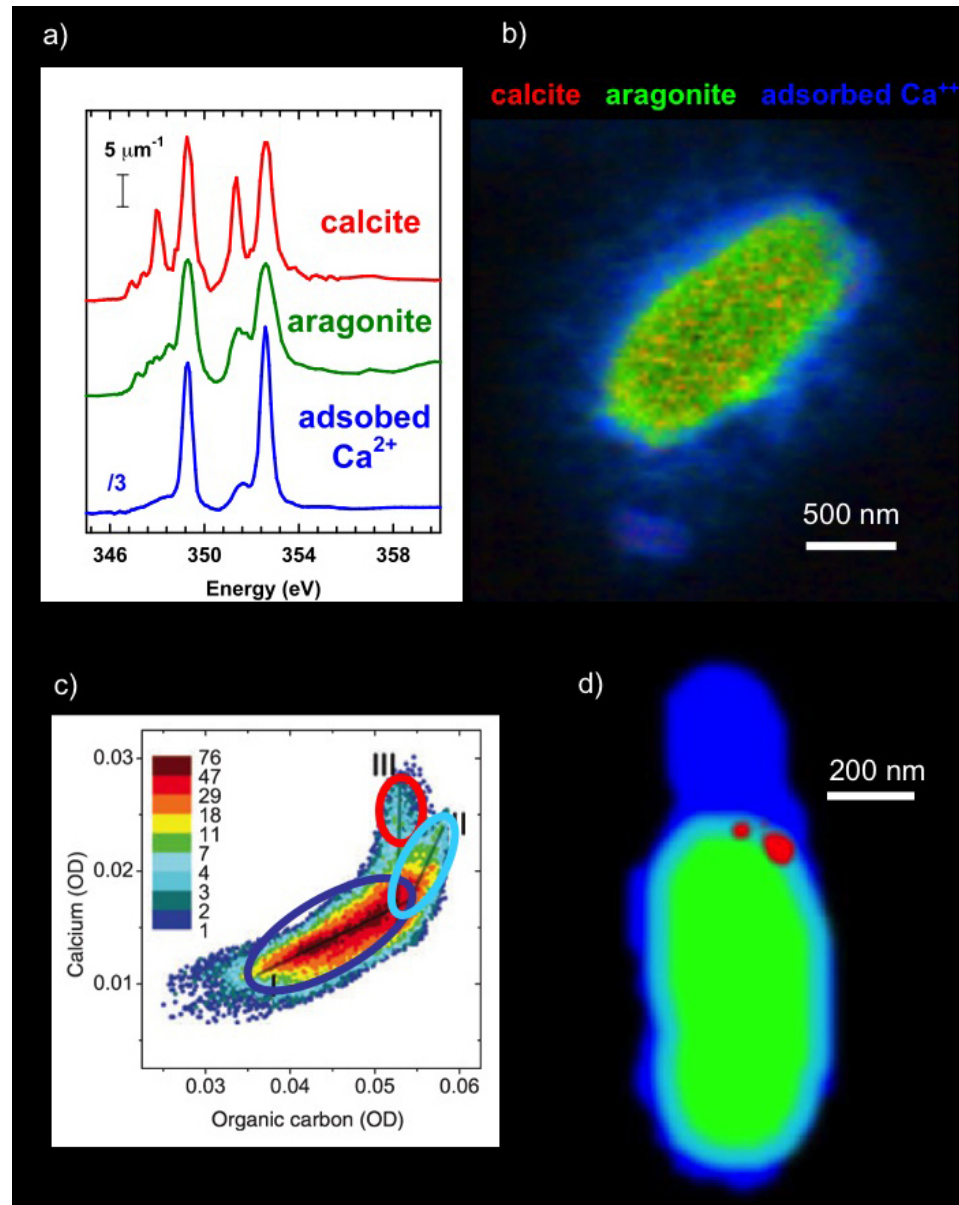
RESULTS

- Ni, Fe, Mn, Ca, K, O, C elemental map, (there was no sign of Cr.)
- Different oxidation states for Fe and Ni



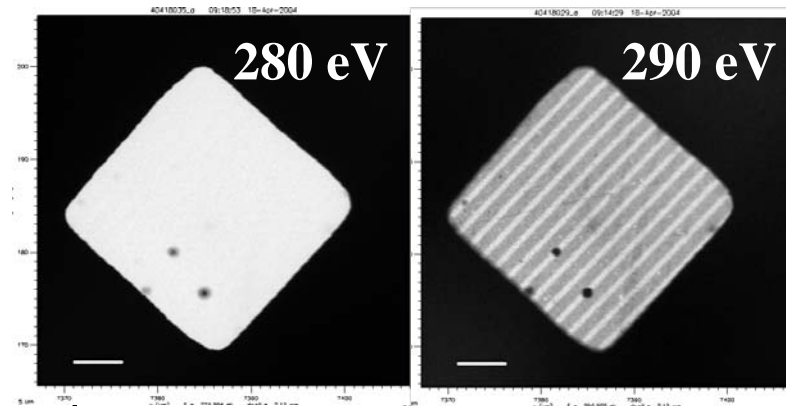
Different oxidation states (minerals) found for Fe & Ni

Tohru Araki, Adam Hitchcock (McMaster University)
Tolek Tyliszczak, LBNL
Sample from: John Lawrence, George Swerhone (NWRI-Saskatoon), Gary Leppard (NWRI-CCIW)

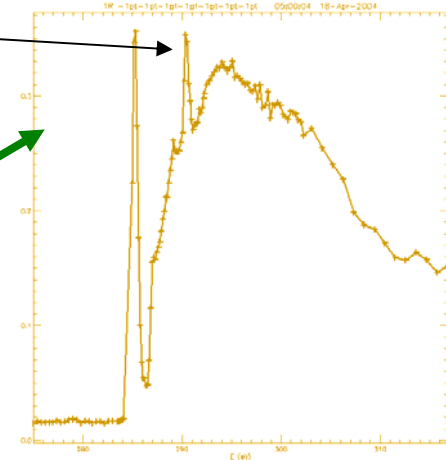
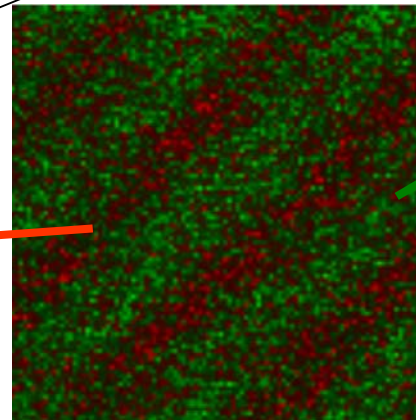
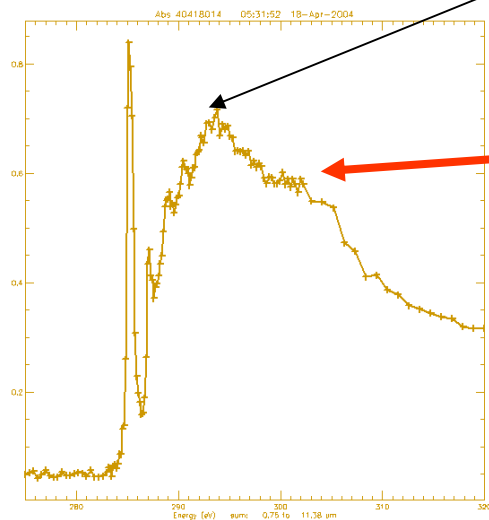


M.K. Gilles, R. Planques, S.R. Leone
LBNL

Samples from B. Hinsberg, F. Huele
IBM Almaden



Exposure to UV light results in loss of carbonyl peak



Map chemical spectra taken of pure samples
onto a sample containing both components

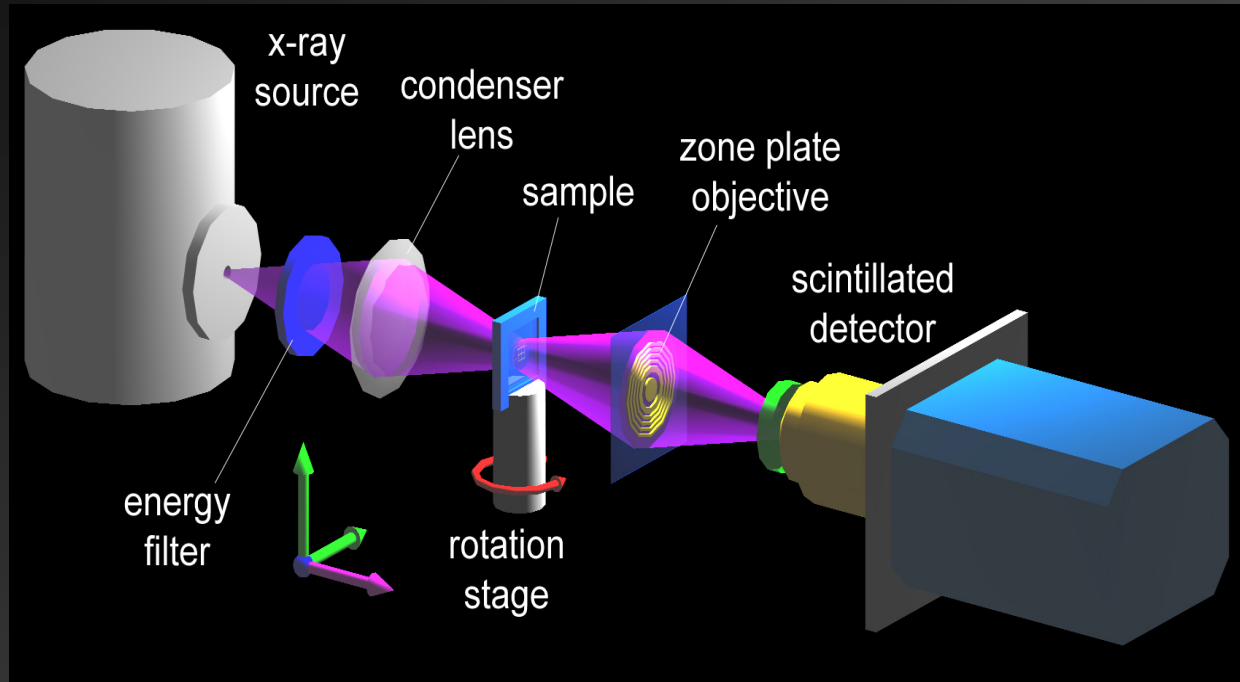
Courtesy of Mary Gilles, LBNL

Hard x-ray zone plate microscopy

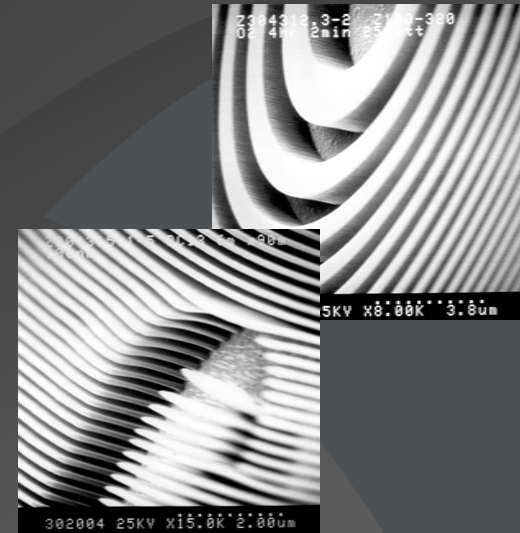


- Shorter wavelengths, potentially better spatial resolution and greater depth-of-field.
- Less absorption (β); phase shift (δ) dominates, higher efficiency.
- Thicker structures required (e.g., zones), higher aspect ratios pose nanofabrication challenges.
- Contrast of nanoscale samples minimal; will require good statistics, uniform background, dose mitigation.

nanoXCT: Schematic and Challenges



X-ray Zone-plate Lens



Challenges for achieving nm scale resolution:

- High resolution objective lens: limiting the ultimate resolution
- High numerical aperture condenser lens:
- Detector: high efficiency for lab. source and high speed for synchrotron sources
- Precision mechanical system

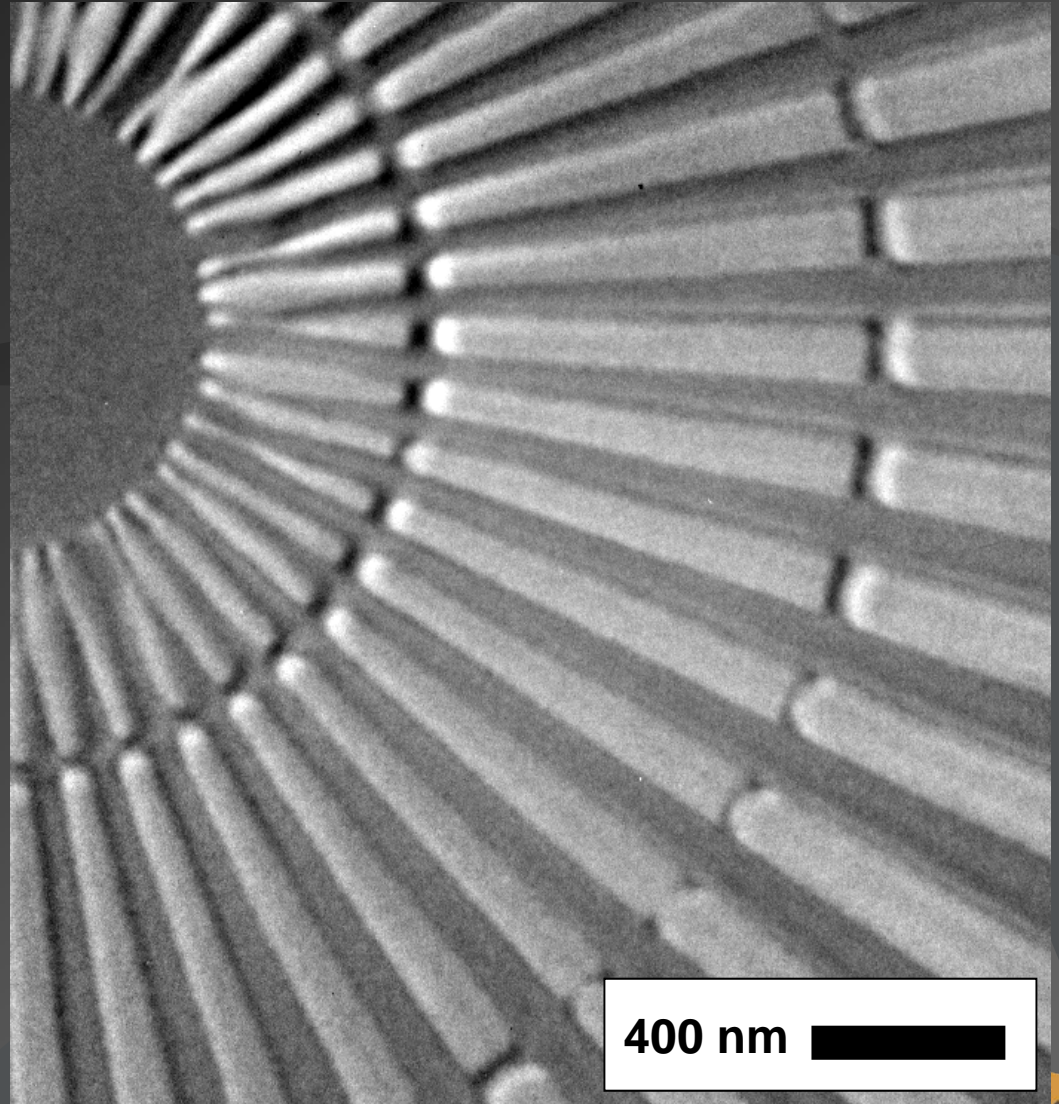
Xradia nanoXCT: Sub-25 nm Hard X-ray Image

Xradia Resolution Pattern

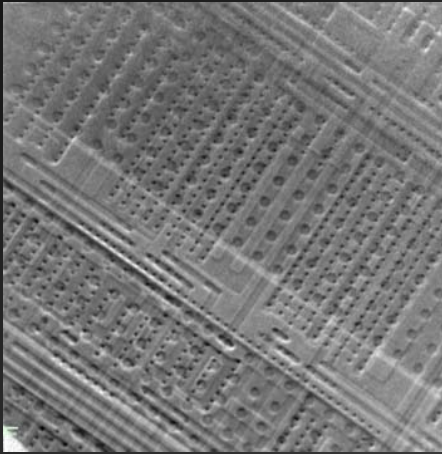
- 50 nm bar width
- 150 nm thick Au
- 8keV x-ray energy
- 3rd diffraction order

F. Duewer, M. Tang,
G. C. Yin, W. Yun,
M. Feser, et al.

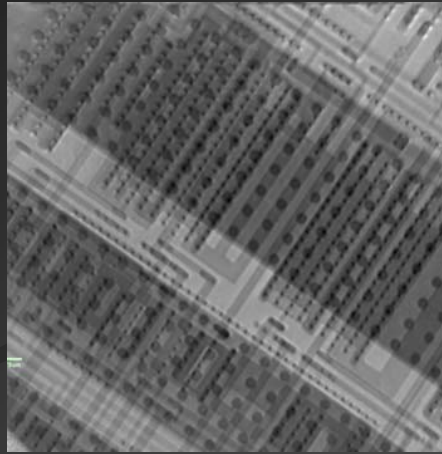
Xradia nano-XCT 8-
50S installed at
NSRRC, Taiwan



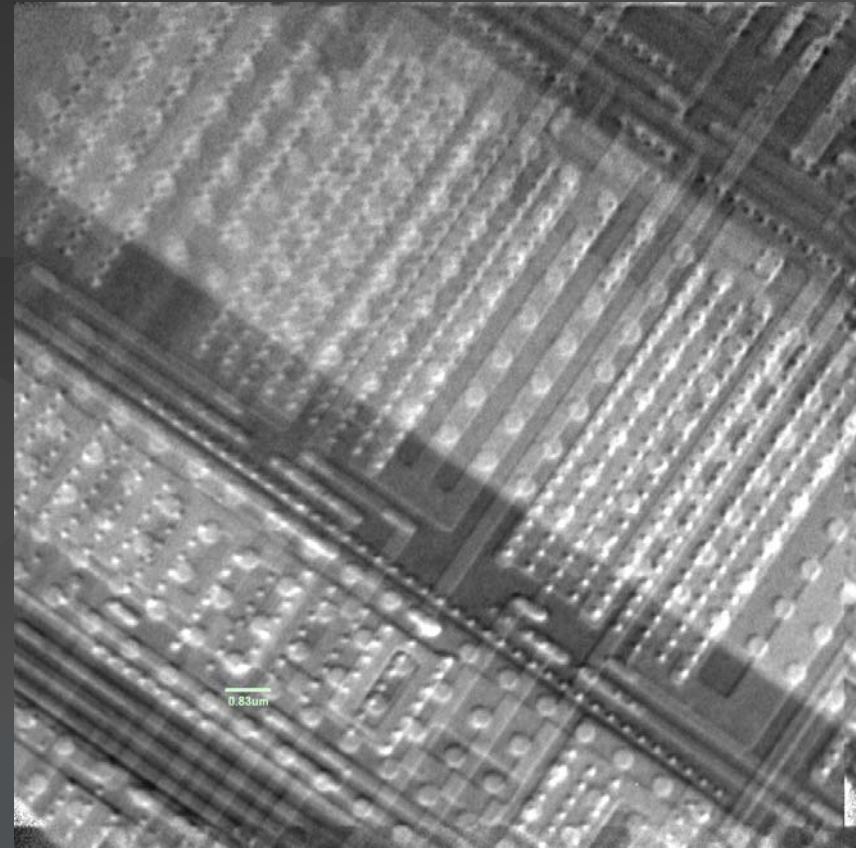
Elemental contrast by tuning energy across the copper absorption edge (Guan-Chian Yin *et al*)



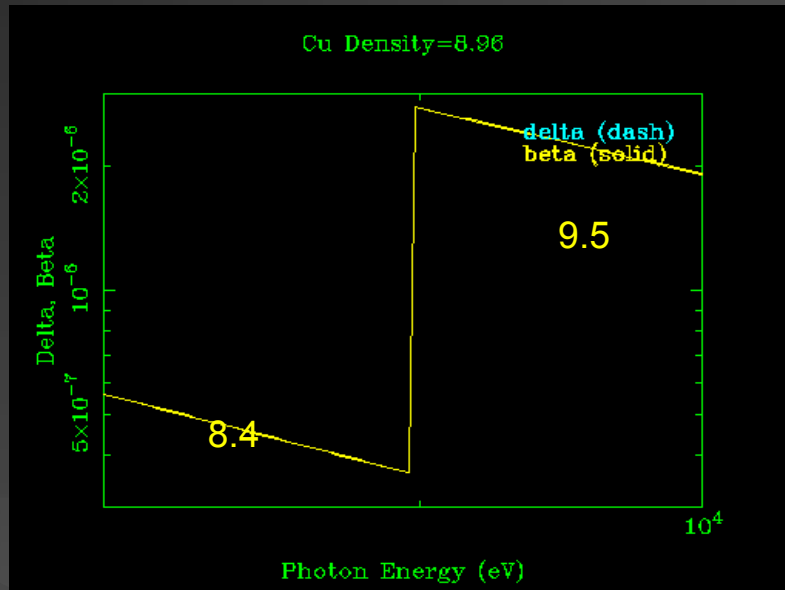
8.4 keV



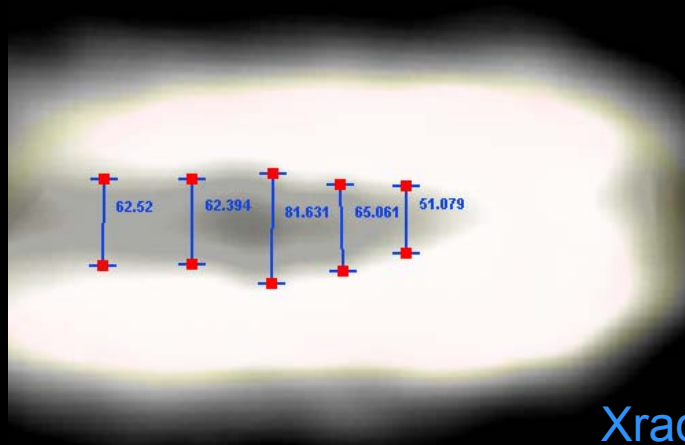
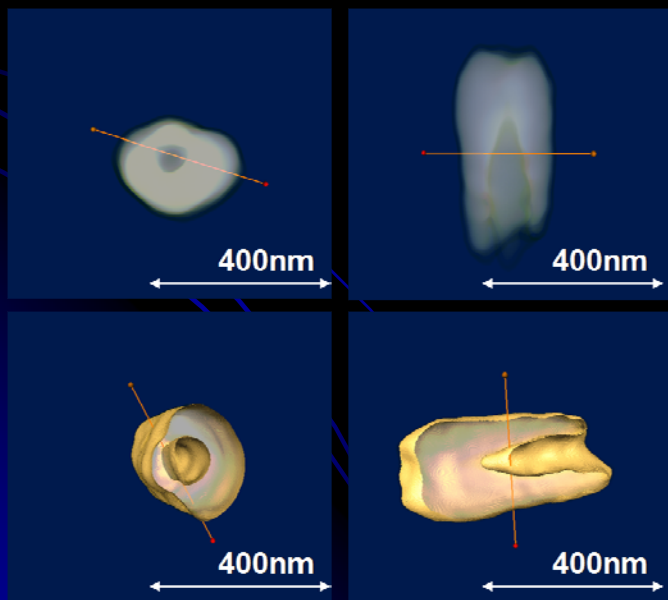
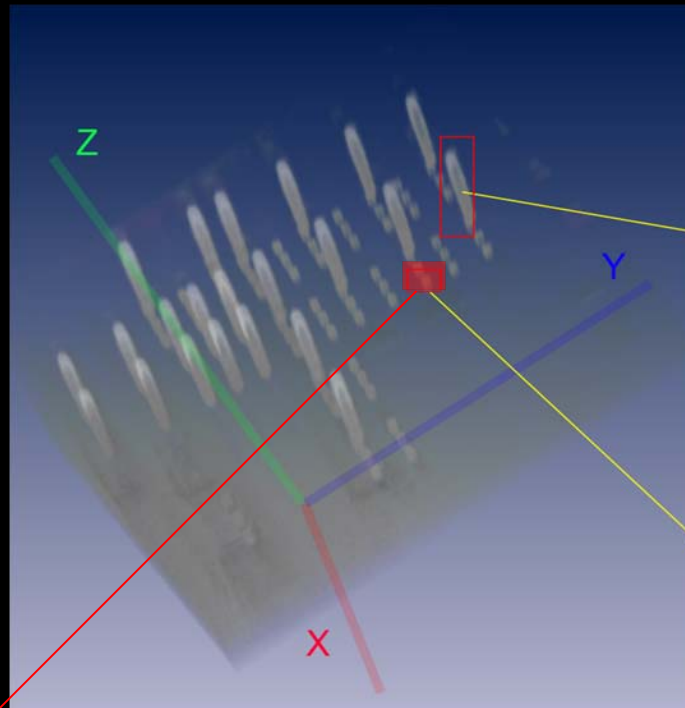
9.5 keV



Intensity difference between
 $E = 8.4 \text{ keV}$ and 9.5 keV

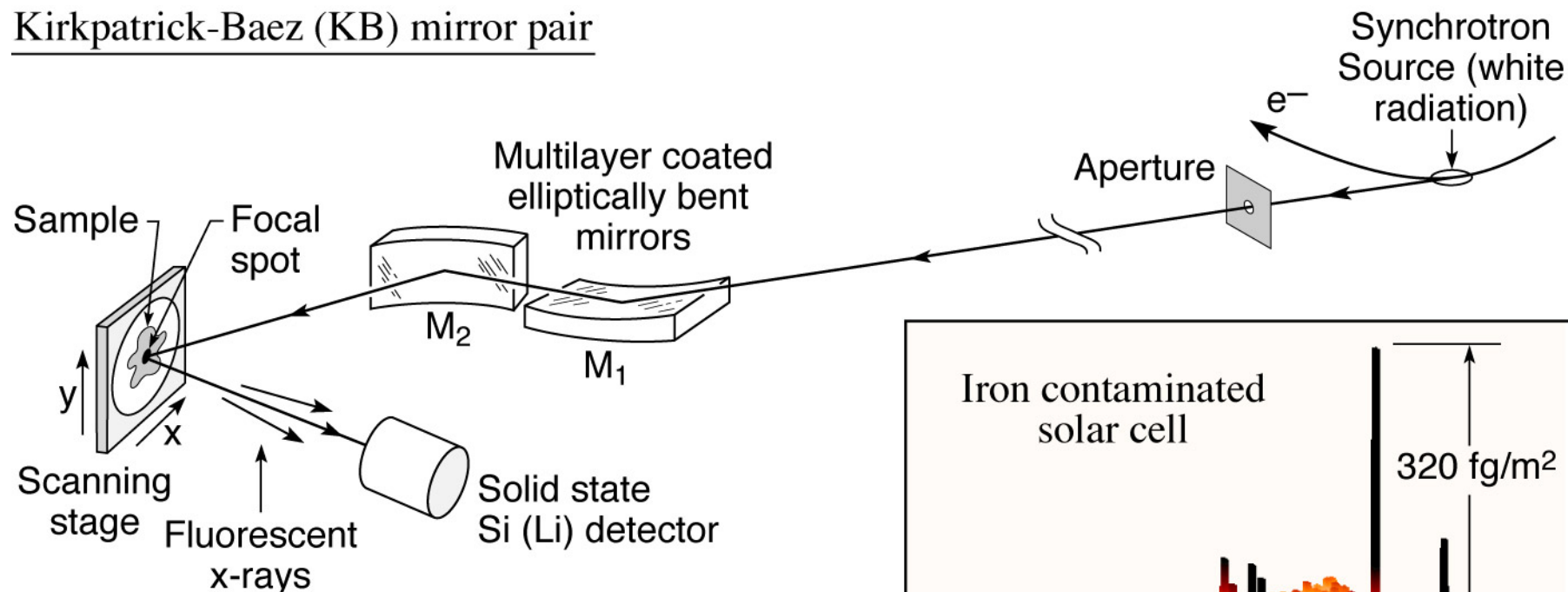


Tomography of a Tungsten plug with "keyhole" at ~60 nm spatial resolution

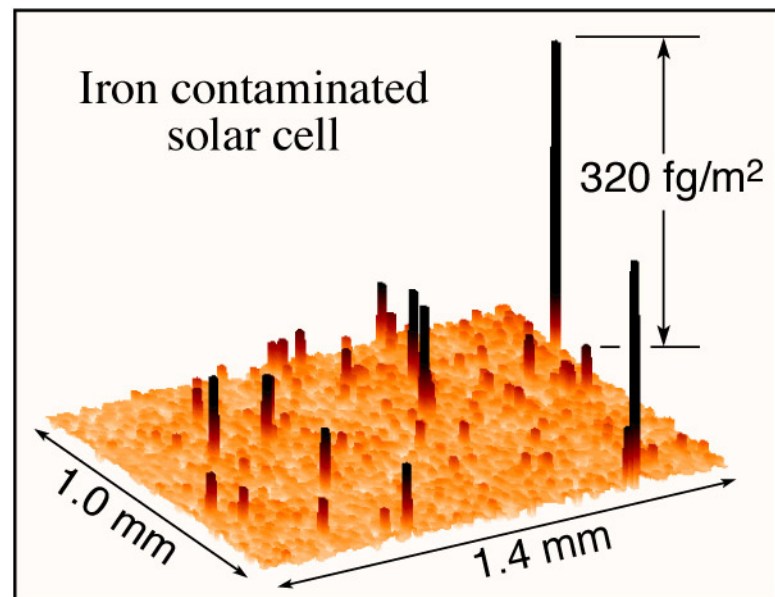


Xradia and NSRRC
APL. 88, 241115 (2006)

Kirkpatrick-Baez (KB) mirror pair



- Crossed cylinders at glancing incidence
- Photon in / photon out, low noise background
- Femtogram and part per billion (ppb) sensitivity
- Micron focus (1988), now ~ 25 nm (Yamauchi, Mimura and colleagues, Osaka U./SPring-8)

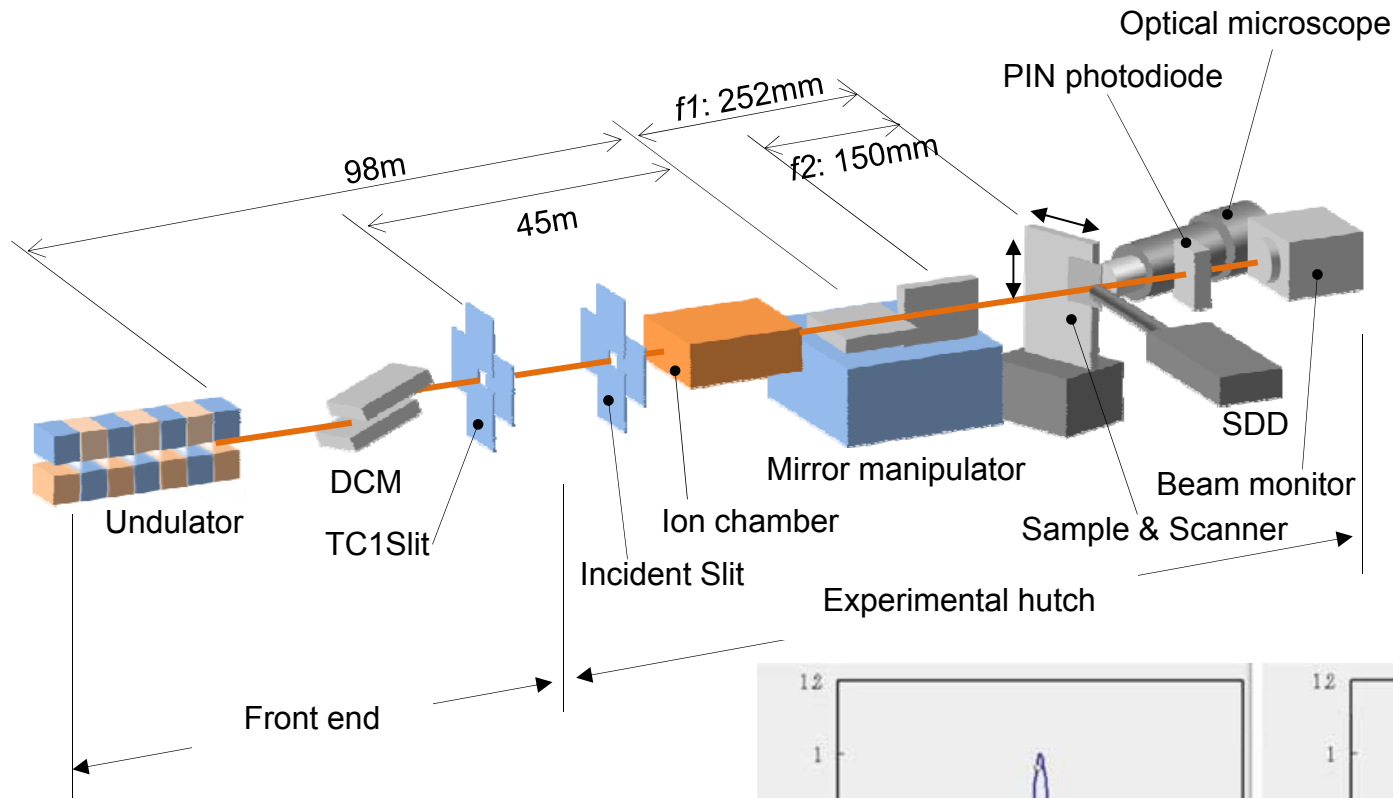


(Courtesy of A. Thompson and J. Underwood, LBNL; and R. Holm, Miles Lab)

FluoresMicroprobe_Sept2010.ai

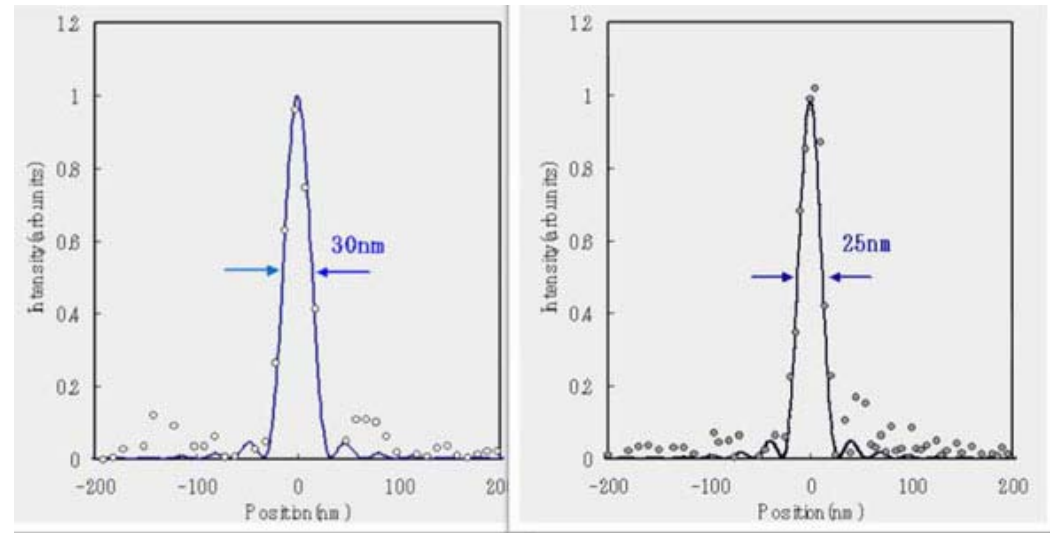
J.H. Underwood and A.C. Thompson, NIM A266, 296 & 318 (1988).

X-ray microprobe at SPring-8

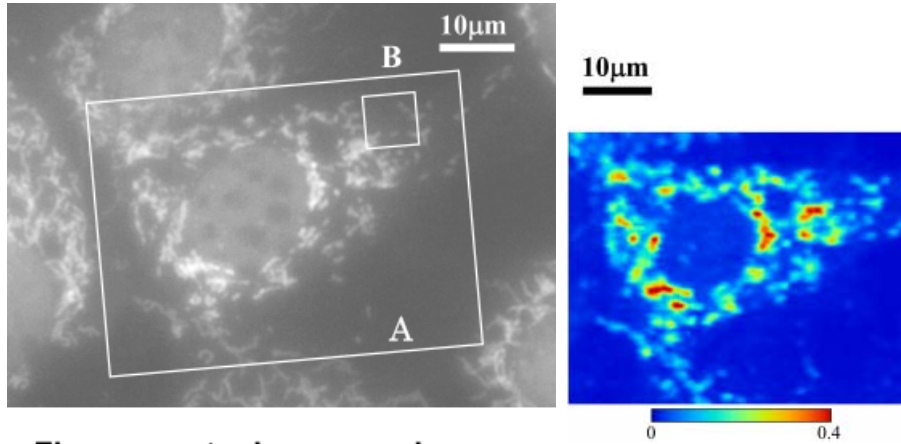


S. Matsuyama et al.,
Rev. Sci. Instrum.
77, 103102 (2006)

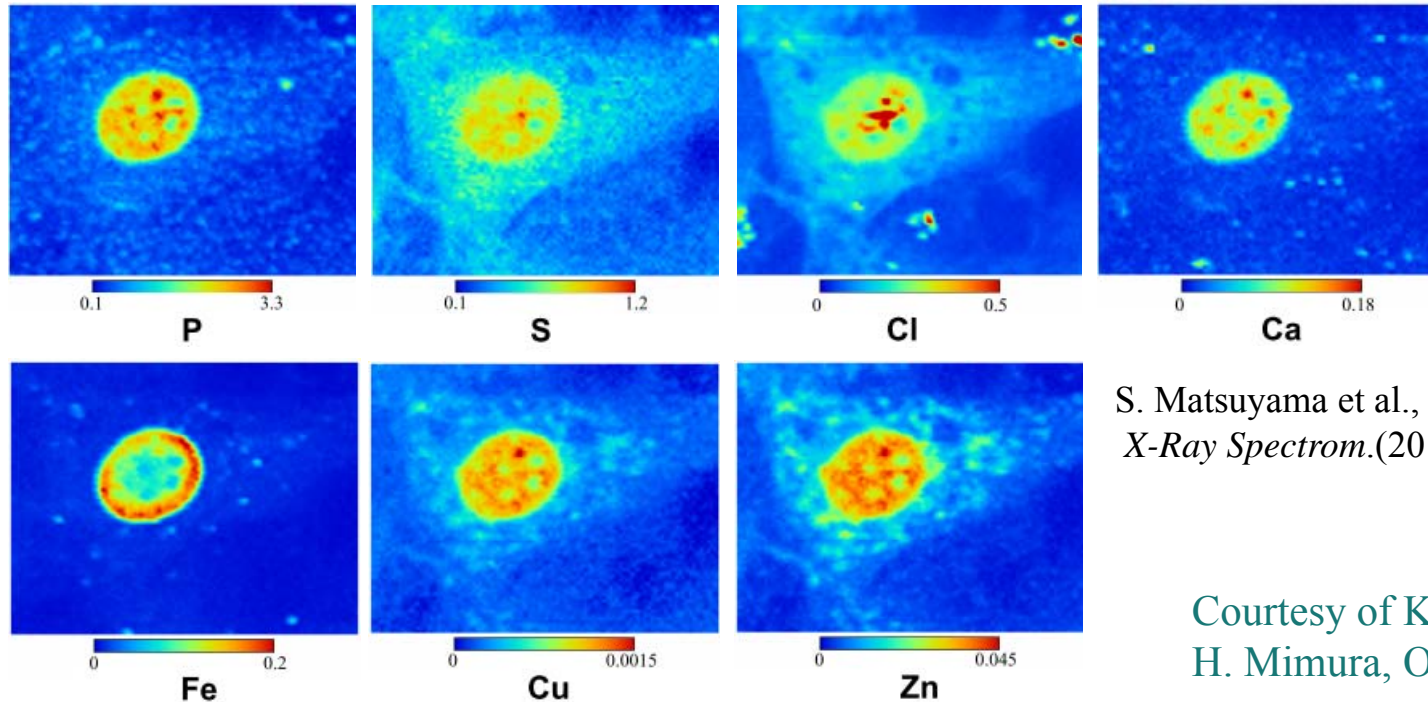
Courtesy of K. Yamauchi and
H. Mimura, Osaka University.



Sub-cellular elemental analysis using the hard x-ray fluorescence microprobe at SPring-8



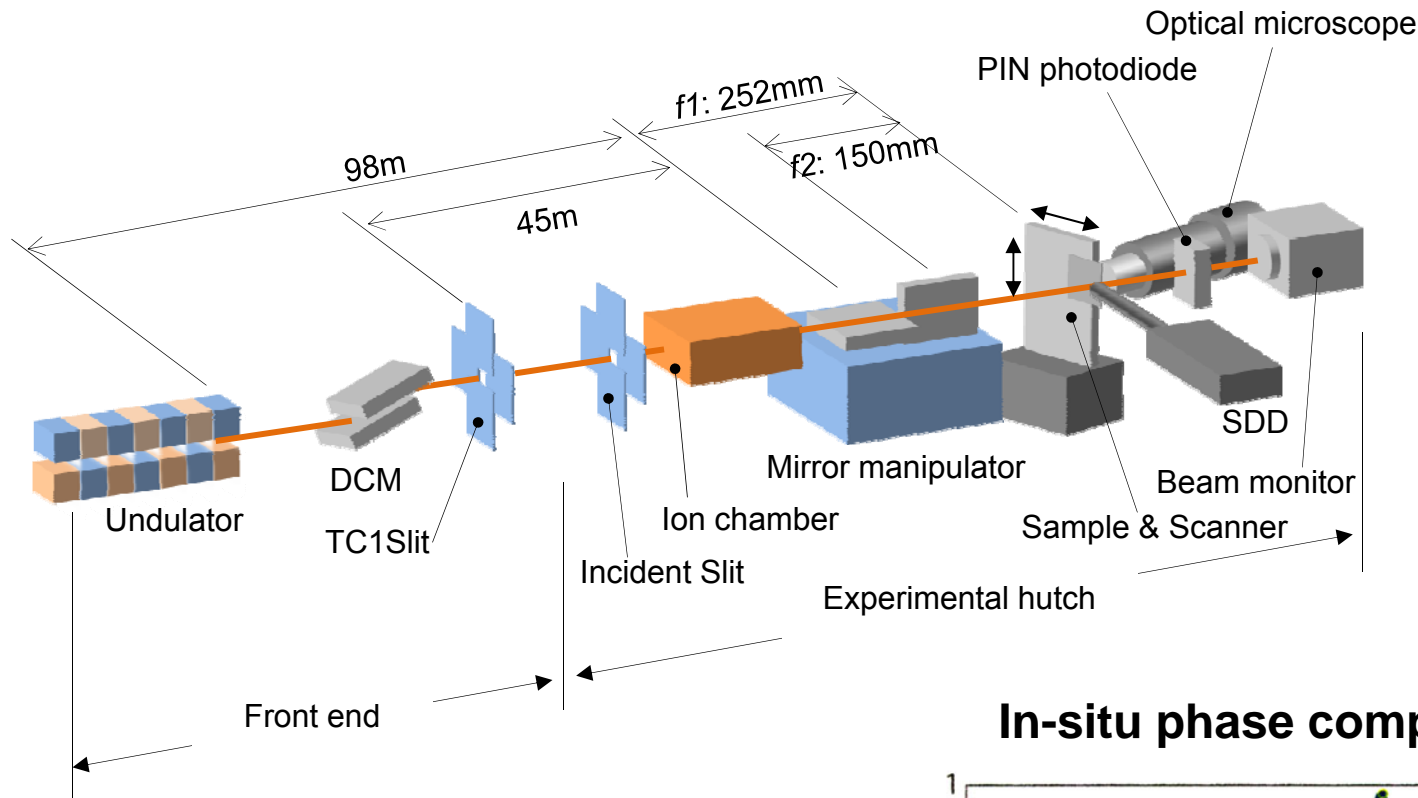
Fluorescent microscope image



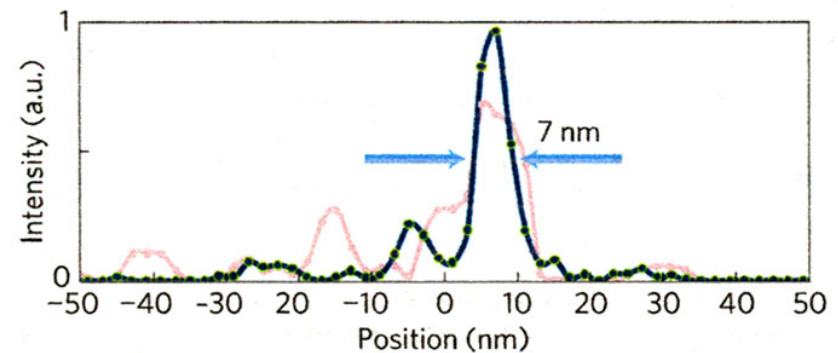
S. Matsuyama et al.,
X-Ray Spectrom.(2010).

Courtesy of K. Yamauchi and
H. Mimura, Osaka University.

X-ray microprobe at SPring-8



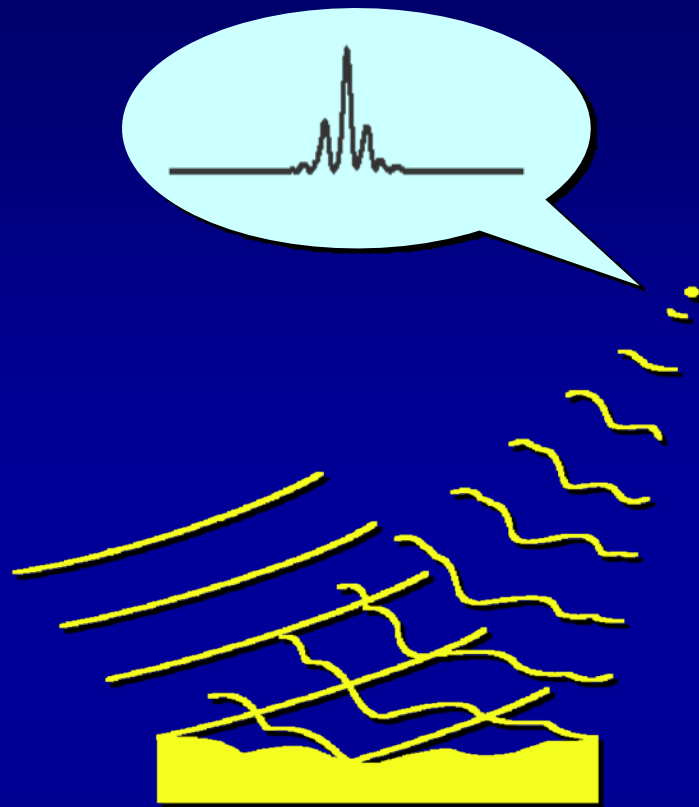
In-situ phase compensation



Courtesy of K. Yamauchi and
H. Mimura, Osaka University.

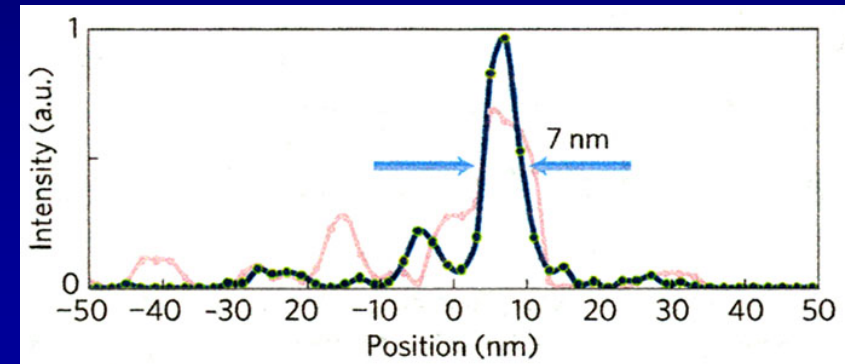
H. Mimura et al., *Nature Physics*, 6, 122 (2009)

Breaking the 10 nm barrier in hard x-ray focusing

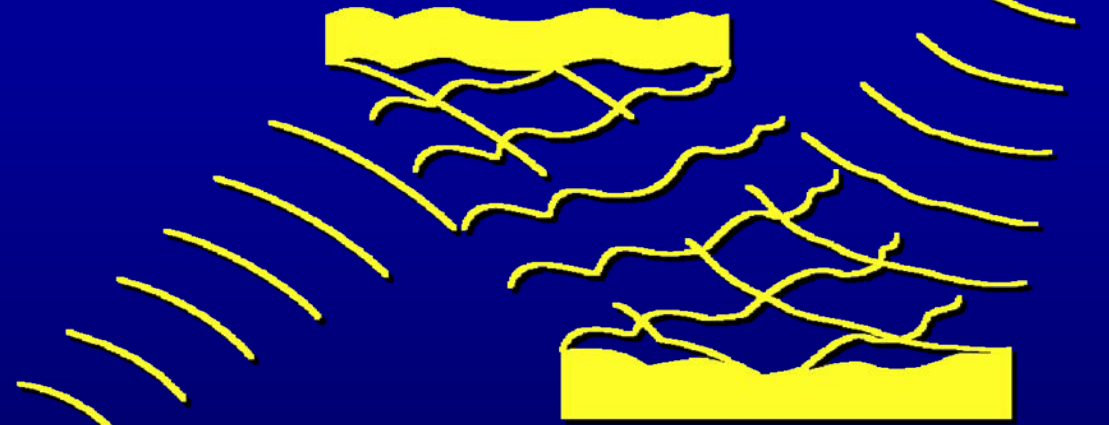


Focusing mirror with phase error

In-situ phase compensation



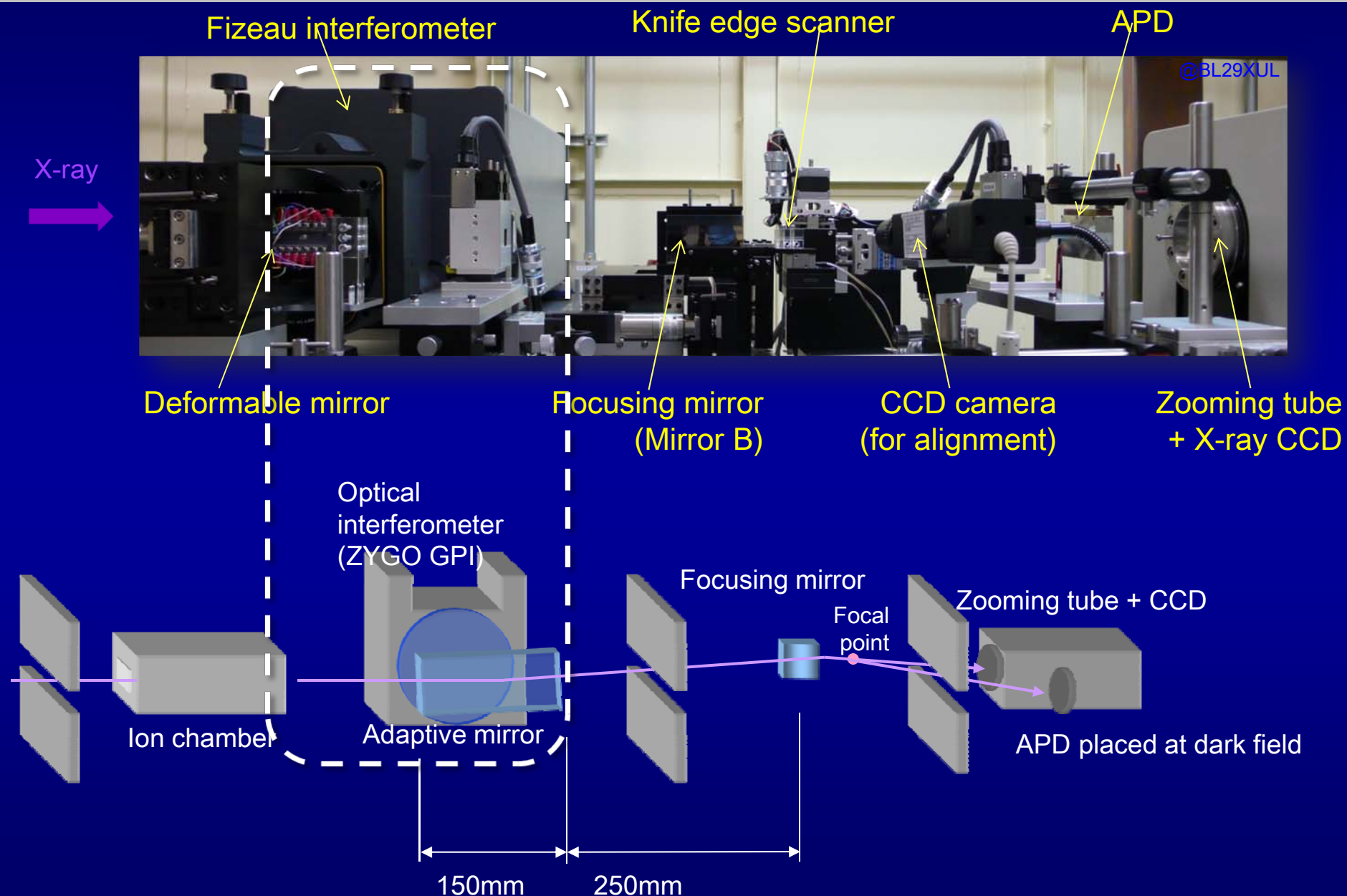
Piezo-electric phase compensator



Focusing mirror with phase error

H. Mimura et al., *Nature Physics*, 6, 122 (2009)

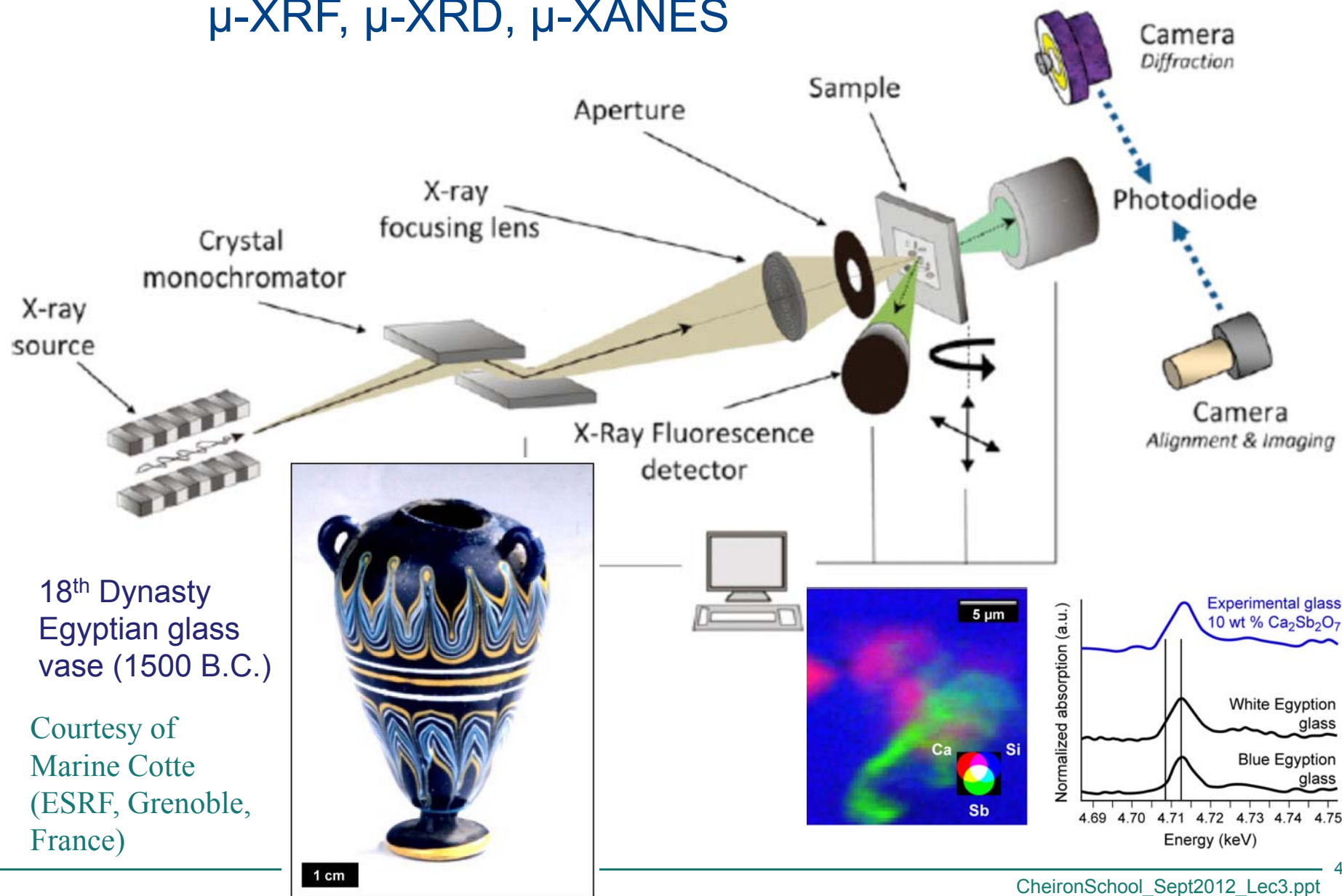
Optical configuration for active phase compensation



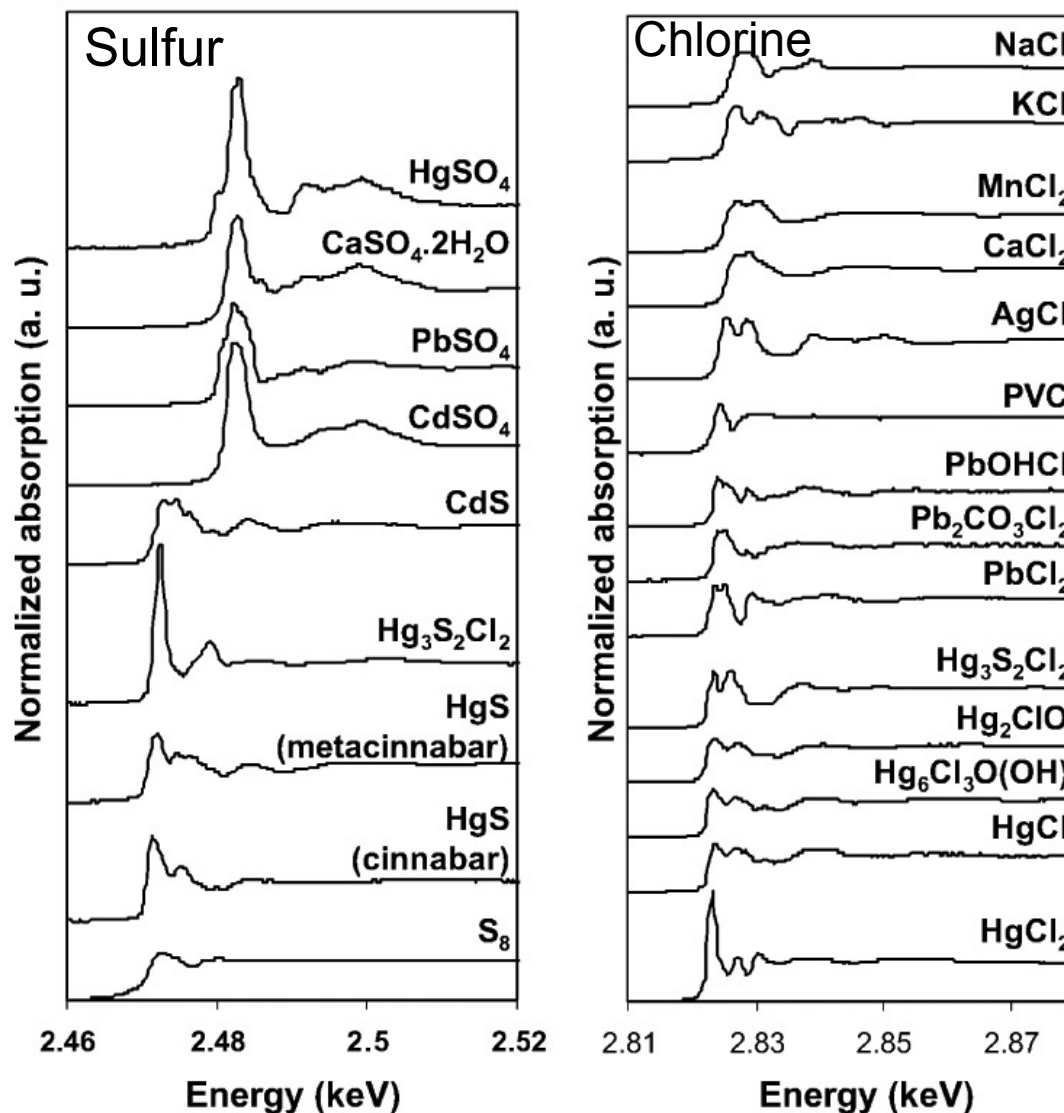
Synchrotron-based art conservation at ESRF



μ -XRF, μ -XRD, μ -XANES



Examples of μ -XANES K-edge spectra occurring in art materials

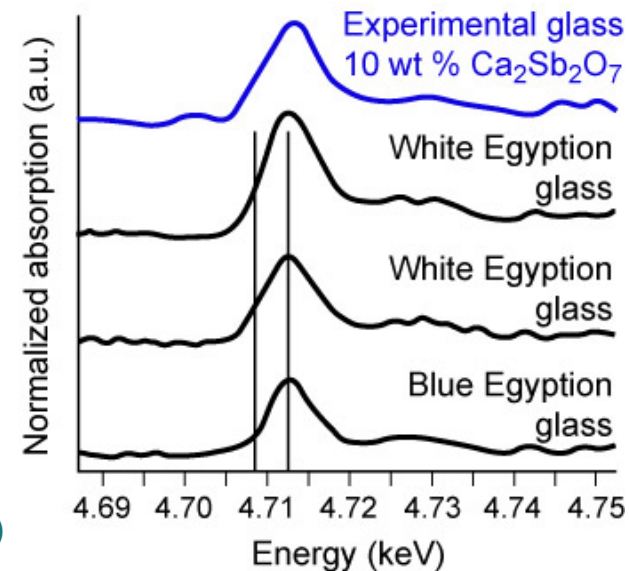
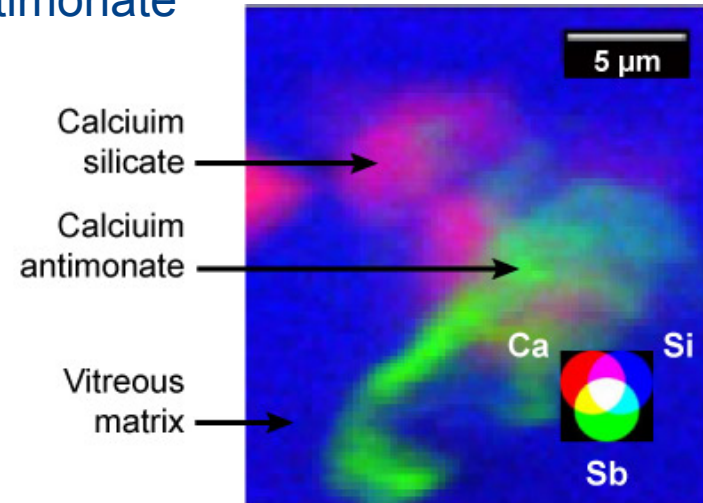


Courtesy of Marine Cotte (ESRF, Grenoble, France)

18th Dynasty Egyptian glass vase studied for an understanding of color and opaqueness in antiquity

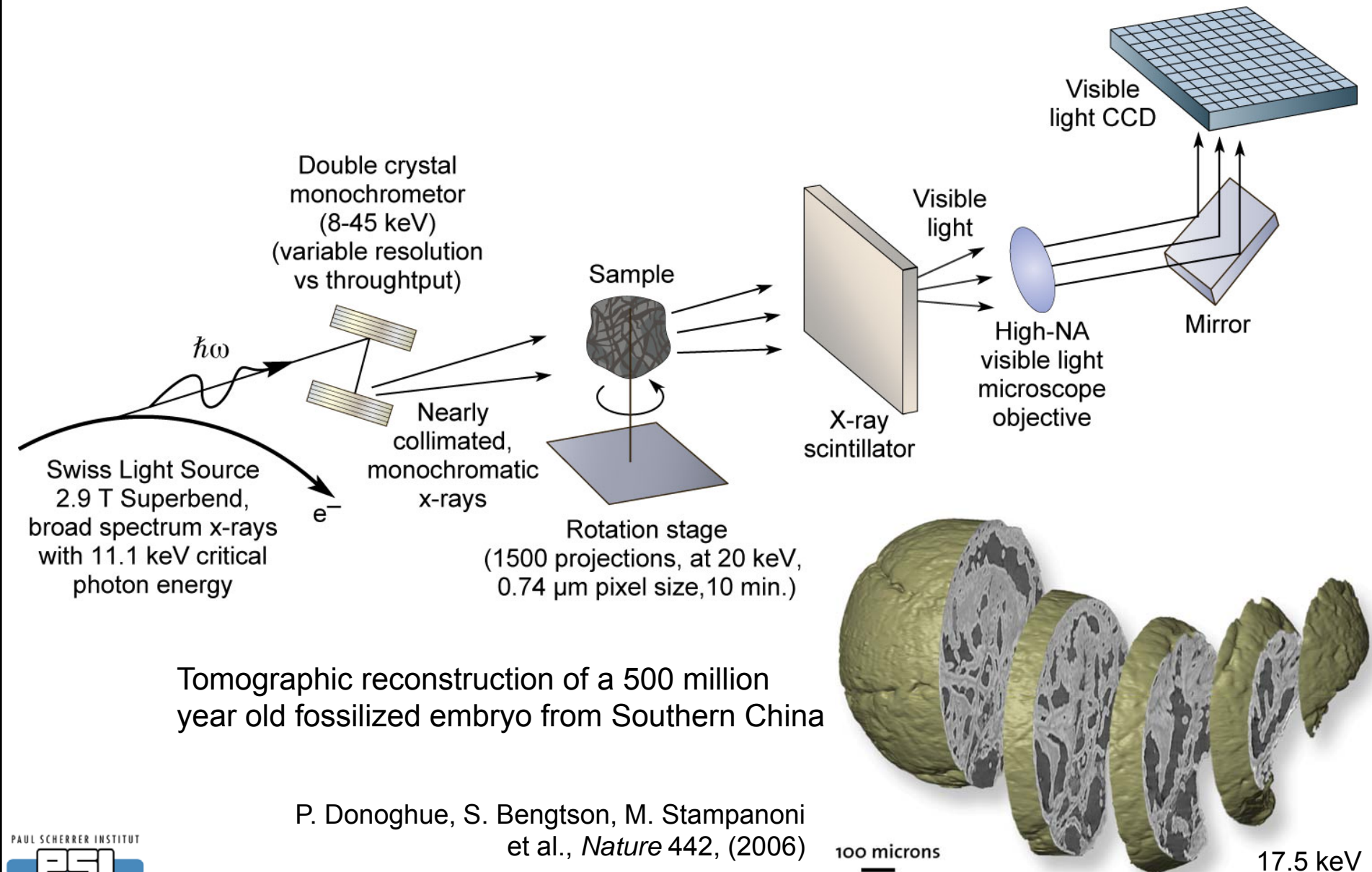


1st production of glass objects Egypt (1500 B.C.),
opaque, colored, nanoscale calcium antimonate



Courtesy of Marine Cotte (ESRF, Grenoble, France)

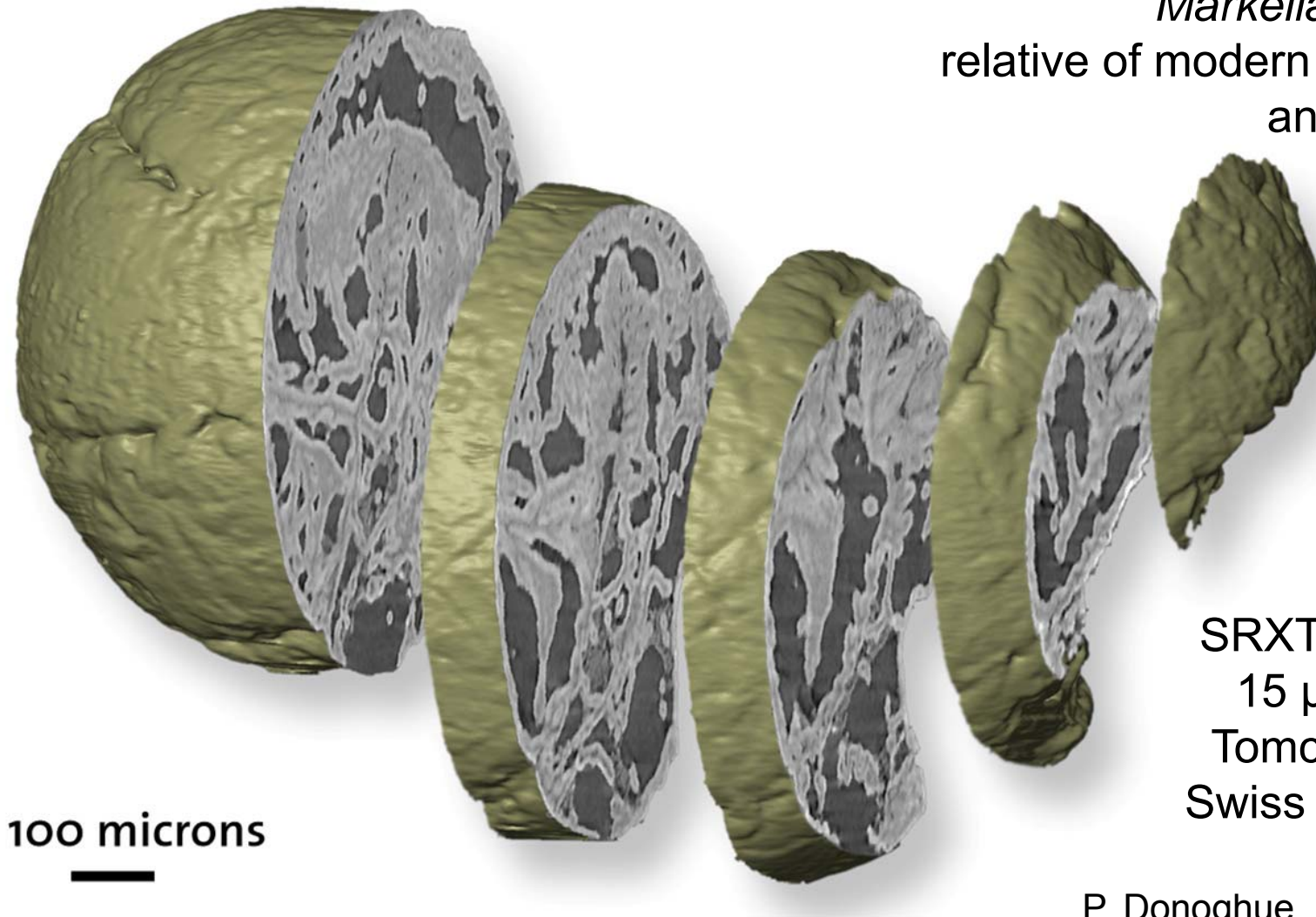
Synchrotron radiation x-ray tomographic microscopy (SRXTM)



P. Donoghue, S. Bengtson, M. Stampanoni
et al., *Nature* 442, (2006)

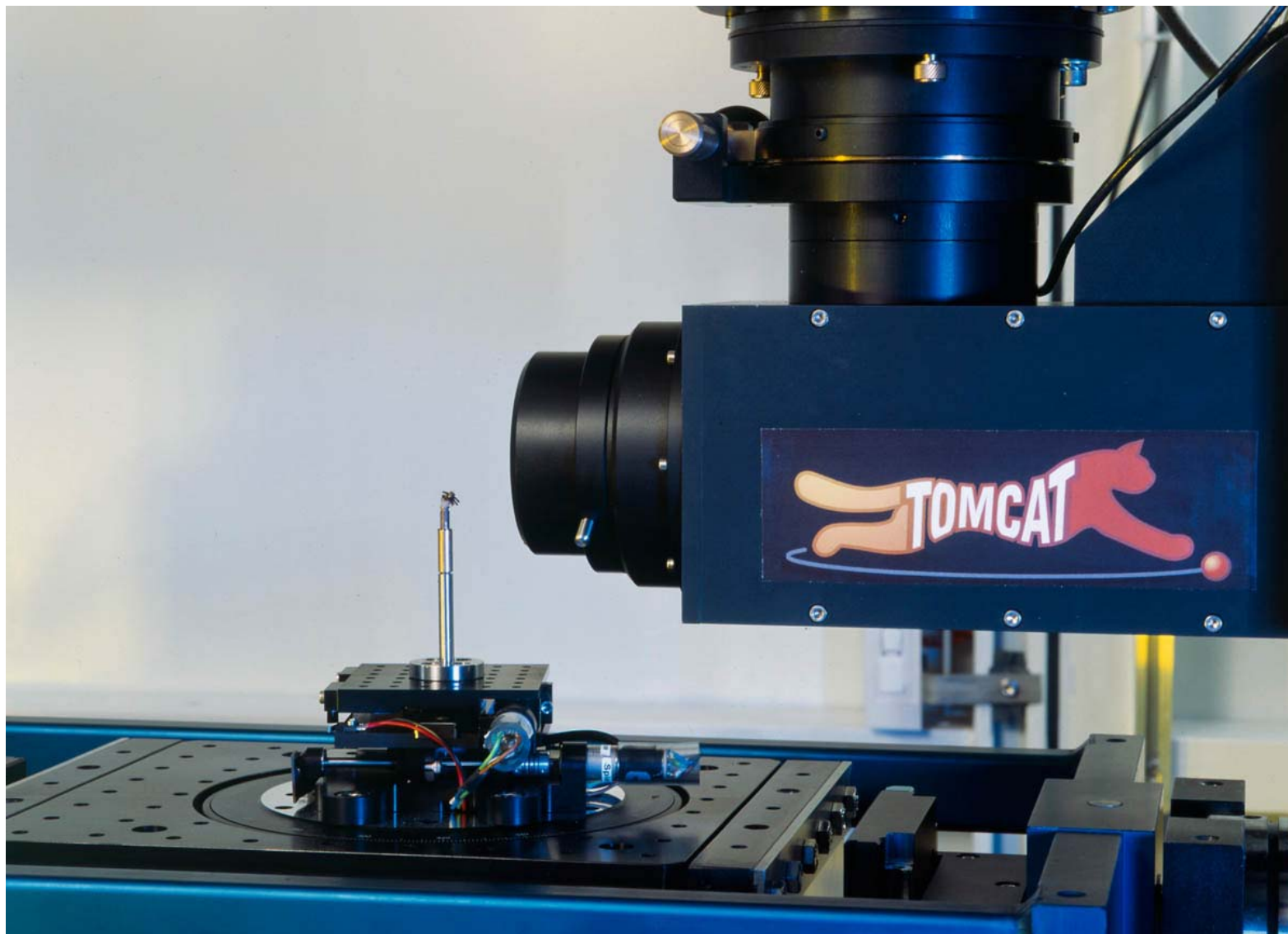
Tomographic reconstruction of a 500 million year old fossilized embryo from Southern China

Markelia hunanensis
relative of modern roundworms
and arthropods



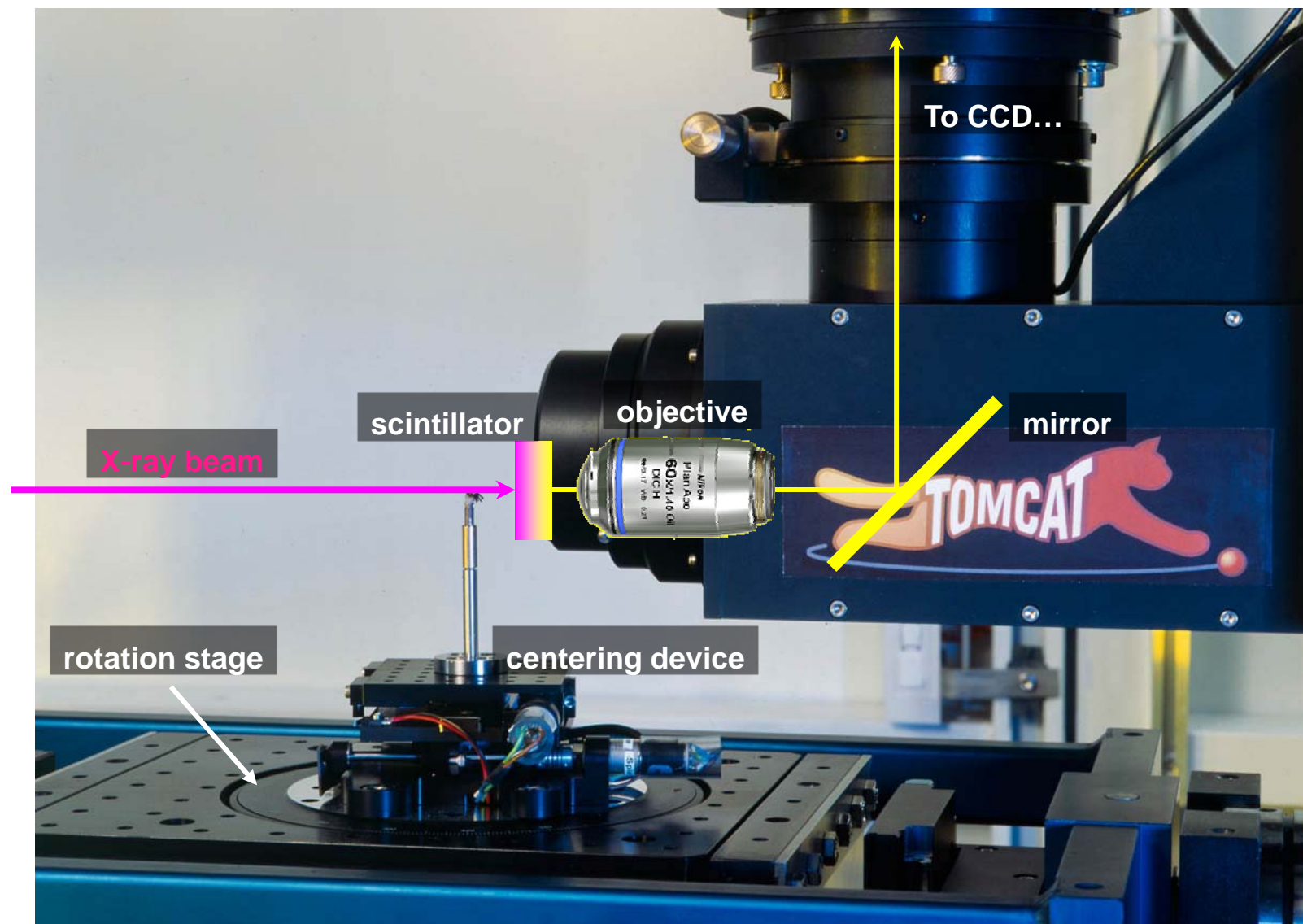
SRXTM, 17.5 keV,
15 μm resolution
Tomcat Beamline,
Swiss Light Source

P. Donoghue, S. Bengtson, M.
Stampanoni et al., *Nature* 442, (2006)



1 micron @ 10% MTF reached routinely

Courtesy of Marco Stampanoni, Swiss Light Source.



1 micron @ 10% MTF reached routinely

Courtesy of Marco Stampanoni, Swiss Light Source.

Hard x-ray 3D x-ray tomography: microvascular architecture of a mouse brain



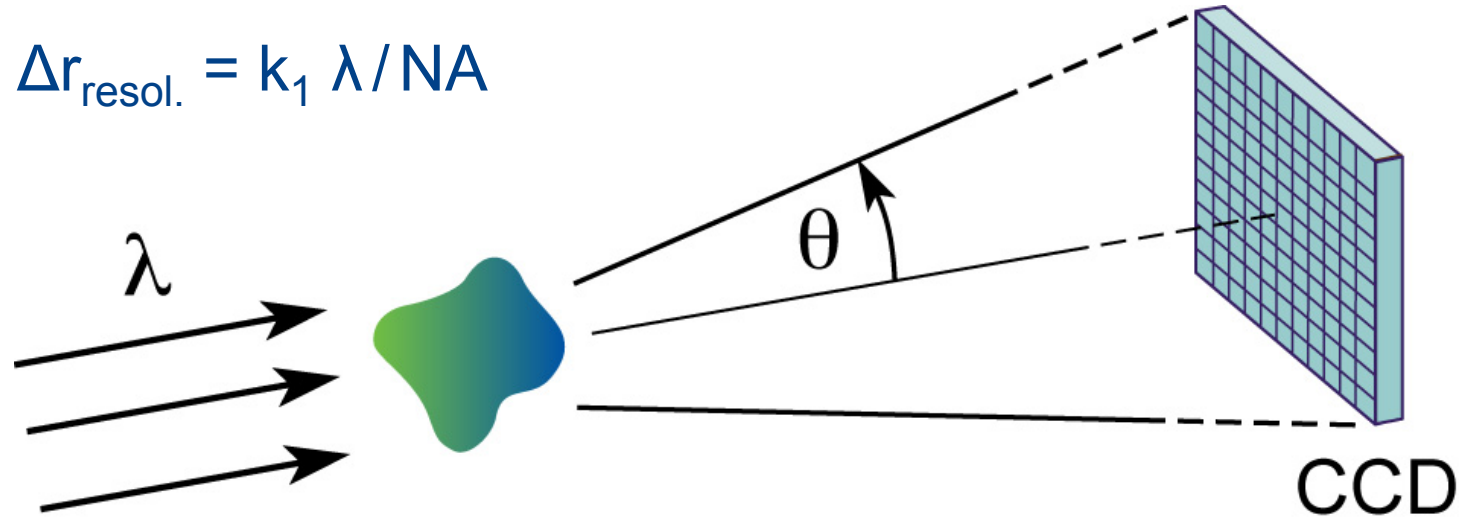
SRXTM, 25 keV,
15 μm resolution
Tomcat Beamline,
Swiss Light Source

M. Stampanoni,
T. Krucker et al.,
Adv. Neur. Res. (2008)

A lens is not necessarily required

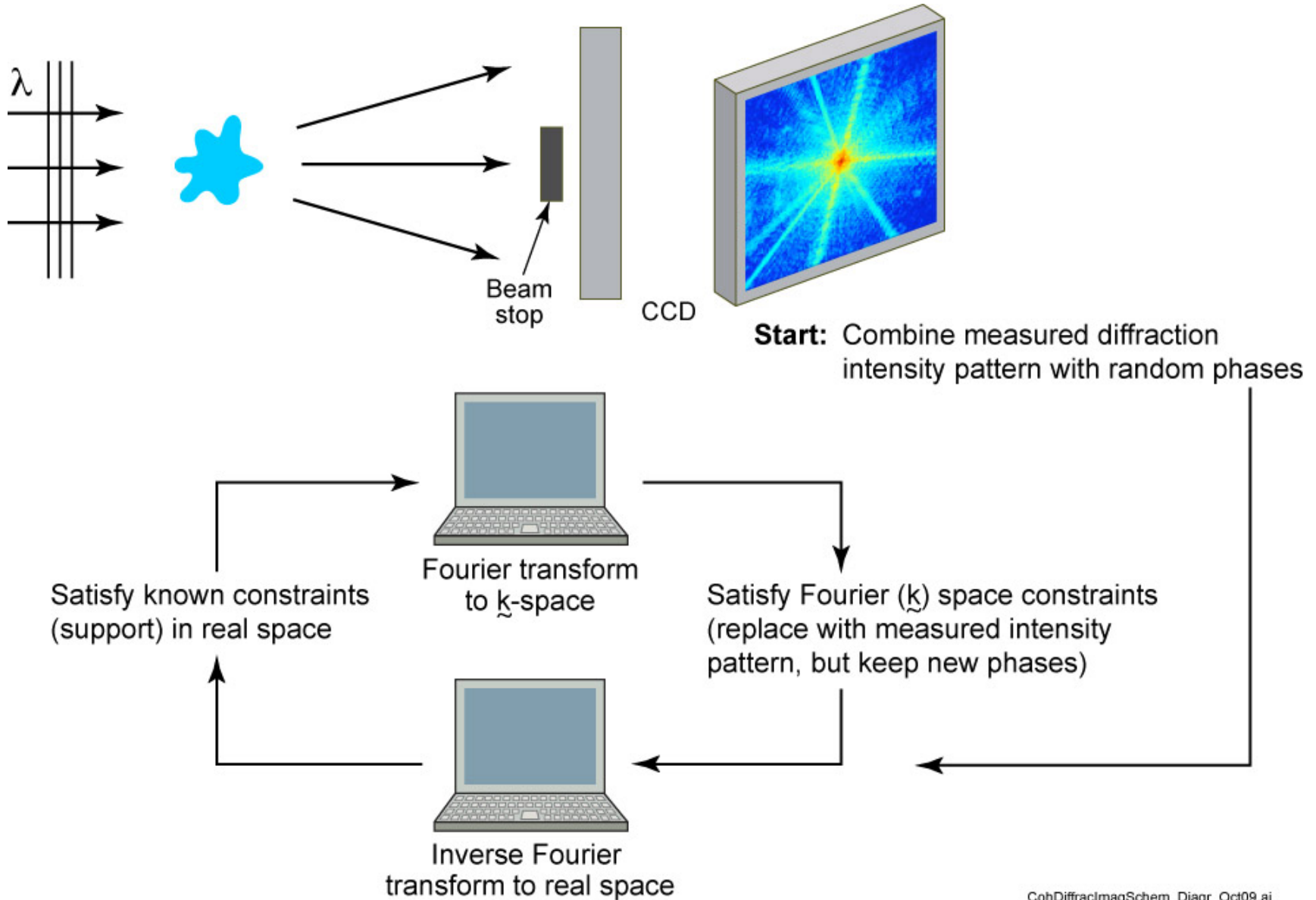


$$\Delta r_{\text{resol.}} = k_1 \lambda / \text{NA}$$



“Lensless” coherent diffraction imaging (CDI) is being aggressively pursued.

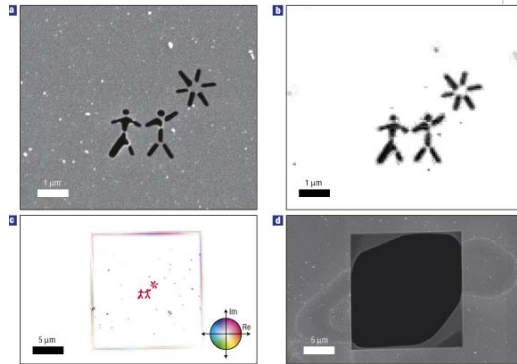
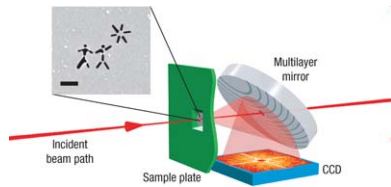
Coherent diffractive imaging (CDI)



Coherent diffractive imaging (CDI) examples



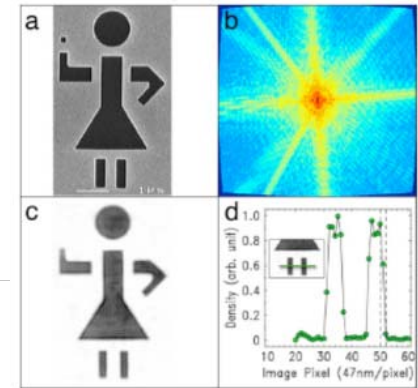
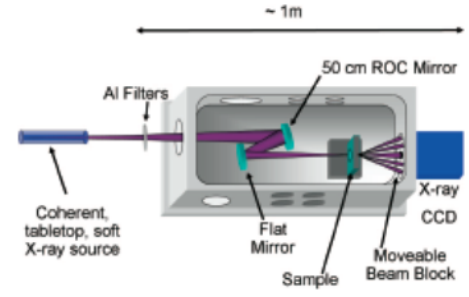
Femtosecond diffractive imaging with a free electron laser



Flash FEL, $\lambda = 32$ nm (39 eV)
25 fsec, 10^{12} photons/pulse
62 nm resolution

Chapman, et al. Nature Physics (2006)

CDI with laboratory scale high harmonic generation (HHG)



HHG, $n = 27$, $\lambda = 29$ nm (43 eV)
94 nm spatial resolution

Sandberg, et al. PNAS (2008)

Synchrotron based CDI of 100 nm Au spheres

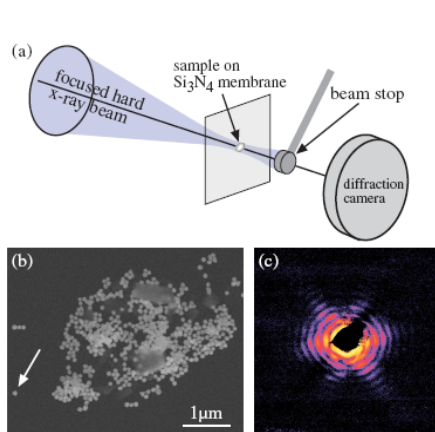


FIG. 1 (color online). (a) Schematic sketch of the coherent diffraction imaging setup with nanofocused illumination. (b) Scanning electron micrograph of gold particles (diameter ≈ 100 nm) deposited on a Si_3N_4 membrane. (c) Diffraction pattern (logarithmic scale) recorded of the single gold particle pointed to by the arrow in (b) and illuminated by a hard x-ray beam with lateral dimensions of about 100×100 nm². The maximal momentum transfer, both in horizontal and vertical direction, is $q = 1.65$ nm⁻¹.

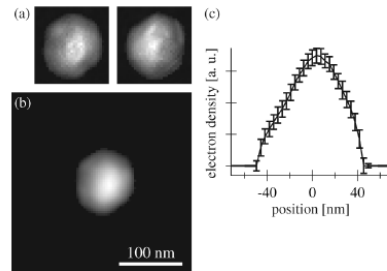
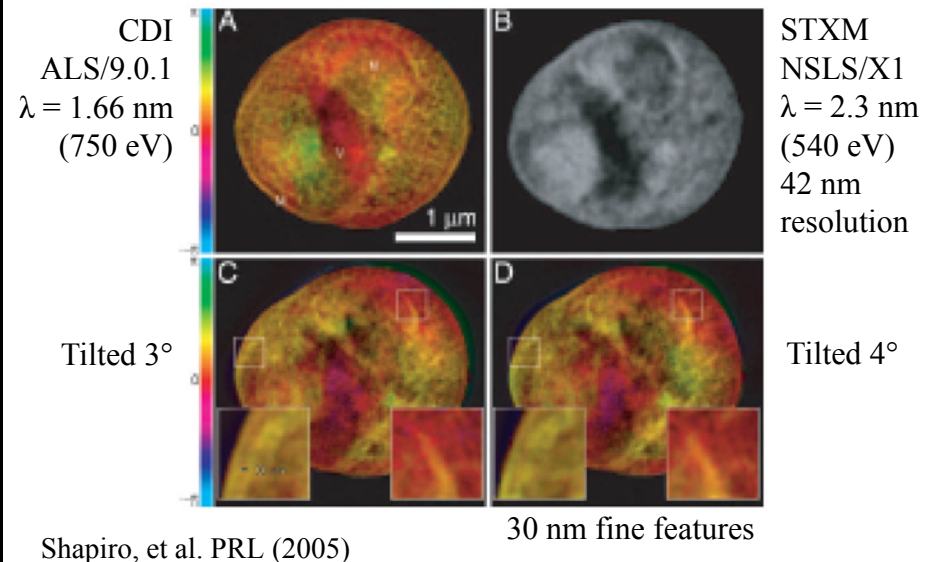


FIG. 2. (a) Two individual reconstructions of the gold particle using the HIO algorithm, a left- and a right-handed one. To obtain the average particle shape from a series of reconstructions with random initial phases, the right-handed reconstructions were inverted and averaged together with the left-handed ones. (b) Reconstructed projected electron density of the gold nanoparticle shown in Fig. 1(b) after averaging the series of reconstructions. (c) Horizontal section through the center of the particle shown in (b). The error bars indicate rms variations in the density for the series of independent reconstructions.

Synchrotron CDI of Au particles
 $\lambda = 0.083$ nm (15 keV),
5 nm “resolution”

Schroer, et al. PRL (2008)

Synchrotron based CDI of a freeze dried yeast cell



CDI
ALS/9.0.1
 $\lambda = 1.66$ nm
(750 eV)

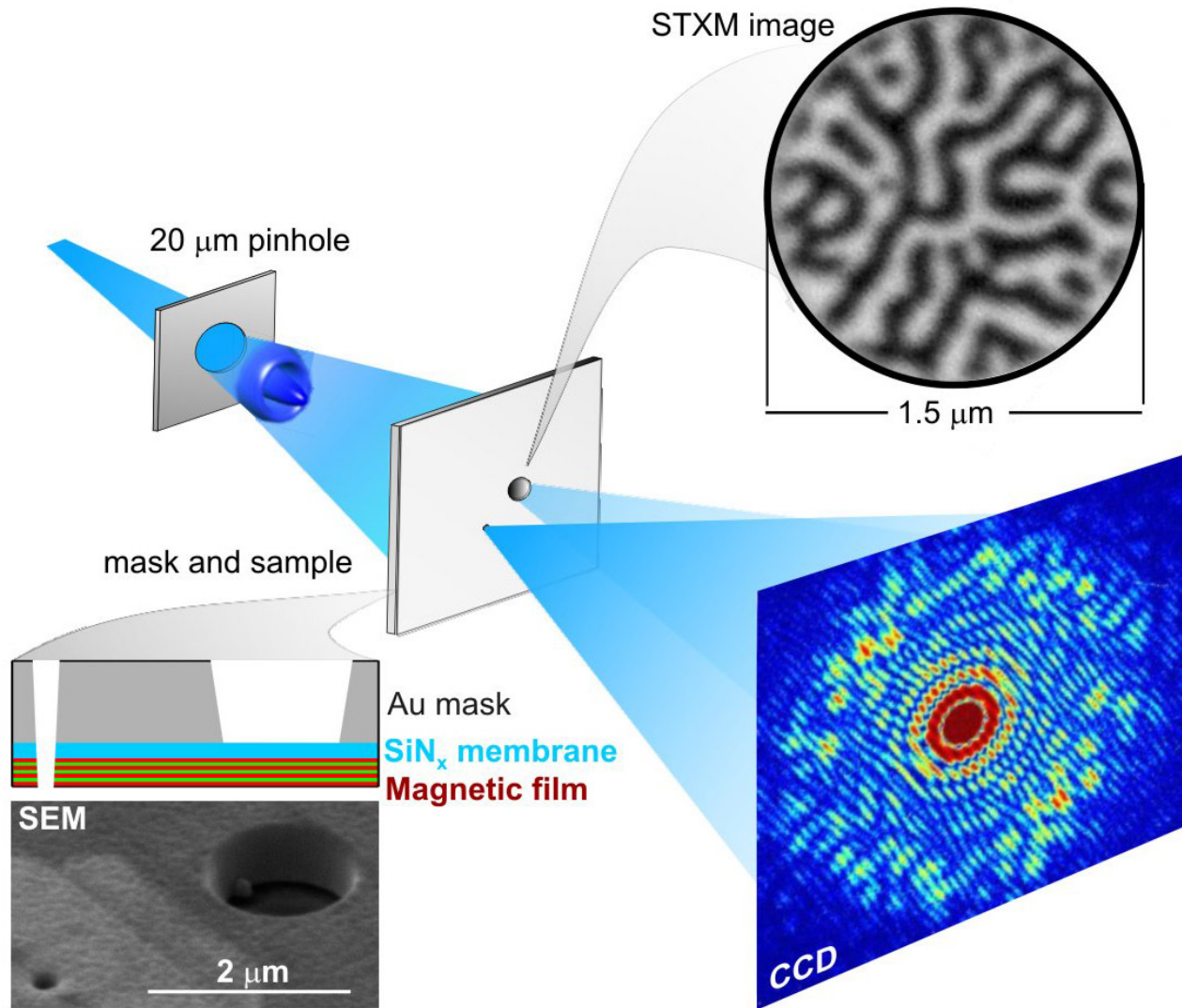
STXM
NSLS/X1
 $\lambda = 2.3$ nm
(540 eV)
42 nm
resolution

Tilted 3°

Tilted 4°

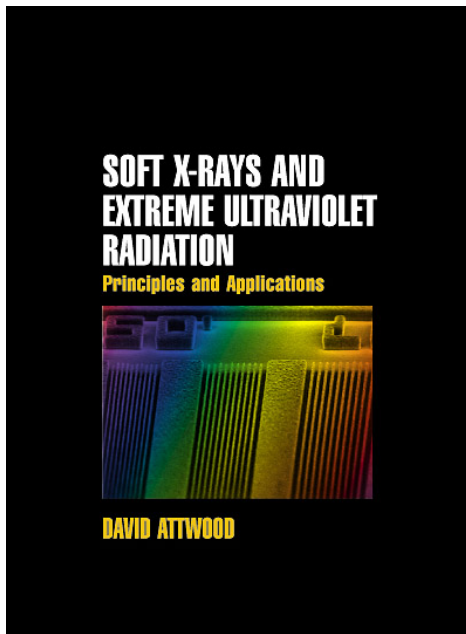
30 nm fine features

Shapiro, et al. PRL (2005)



S. Eisebitt, J. Lüning, W.F. Schlotter, M. Lörger, O. Hellwig,
W. Eberhardt & J. Stöhr / *Nature*, 16 Dec 2004

LenslessImagingF1.ai



Amazon.com



UC Berkeley

www.coe.berkeley.edu/AST/sxreuv

www.coe.berkeley.edu/AST/srms

www.coe.berkeley.edu/AST/sxr2009